This manuscript was accepted by Phys. Fluids. Click here to see the version of record.

Rayleigh-Taylor Instability of a Miscible Interface in a Confined Domain

T. Lyubimova,[1,2] A. Vorobev,[3,a)] and S. Prokopev[1]

[1)] *Institute of Continuous Media Mechanics UB RAS, Perm, 614013, Russia*

[2)] *Perm State University, Perm, 614990, Russia*

[3)] *Faculty of Engineering and Physical Sciences, University of Southampton, Southampton, SO17 1BJ, UK*

(Dated: 11 December 2018)

On the basis of the phase-field approach we investigate the simultaneous diffusive and convective evolution of an isothermal binary mixture of two slowly miscible liquids that are confined in a horizontal plane layer. We assume that two miscible liquids are brought into contact so the binary system is thermodynamically unstable and the heavier liquid is placed on top of the lighter liquid so the system is gravitationally unstable. Our model takes into account the non-Fickian nature of the interfacial diffusion and the dynamic interfacial stresses at a boundary separating two miscible liquids. The numerical results demonstrate that the classical growth rates that characterise the initial development of the Rayleigh-Taylor instability can be retrieved in the limit of the higher Peclet numbers (weaker diffusion) and thinner interfaces. The further nonlinear development of the Rayleigh-Taylor instability, characterised e.g. by the size of the mixing zone, is however limited by the height of the plane layer. On a longer time scale the binary system approaches the state of thermodynamic and hydrodynamic equilibrium. In addition, a novel effect is found. It is commonly accepted that the interface between the miscible liquids slowly smears in time due to diffusion. We however found when the binary system is subject to hydrodynamic transformations the interface boundary stretches so its thickness changes (the interface becomes thinner) on a much faster convective time scale. The thickness of the interface is inversely proportional to the surface tension, and the stronger surface tension limits the development of the Rayleigh-Taylor instability.

ACCEPTED MANUSCRIPT

I. INTRODUCTION

The mixing control in a system of two miscible fluids that is enclosed in a confined domain is an important engineering problem. The fast and complete mixing is a frequent pre-requirement for improved chemical engineering processes. In this case, the mixing may be enhanced by heating or mechanical agitation, that intensifies the mass transfer or even breaks the phase continua into smaller blobs (droplets) thus enlarging the contact area between the phases. The mixing can be intensified by taking advantage of some hydrodynamic instabilities such as the Kelvin-Helmholtz instability or the Rayleigh-Taylor instability. In other cases, however, development of hydrodynamic instabilities (e.g. viscous fingering) in a miscible system is undesirable,[1,2] and an expected stabilisation of hydrodynamic instabilities may not be achieved[3].

For instance, the process of benzene alkylation, that is used for manufacturing of ethylbenzene, a key intermediate to styrene that in turn is a precursor to polystyrene, can be catalysed by a mineral (Lewis) acid.[4] Benzene and catalyst are fed into the chemical reactor in the liquid forms through a pre-mixing inlet pipe. The ultimate molecular-level mixing of benzene and catalyst occurs rather slowly due to low diffusion coefficients in liquids. The substances enter the pre-mixing pipe through the different inlet openings, and the arrangement of the inlets was found to be quite important. The catalyst is denser than benzene, and thus the injection of benzene above the catalyst slows down the mixing even further, as the liquids become segregated with even slower diffusive interchange through the contact boundary. The injection of the heavier catalyst on top of the benzene phase seems to be more promising, as the similar arrangement is subject to the Rayleigh-Taylor instability that naturally mixes up the phases. In this work we aim to consider the mutual effects of the diffusion on the development of the Rayleigh-Taylor instability and the influence of the instability on the enhancement of the (molecular-level) mixing of the liquids.

The Rayleigh-Taylor instability occurs when a denser liquid is placed on top of a lighter liquid. The linear theory of the Rayleigh-Taylor instability developed in a number of classical works[5,6] shows that for a flat immiscible interface separating two liquids with negligibly low viscosities the amplitude of normal perturbations grows exponentially with the growth rate given by the expression,

$$\omega^2 = g\frac{\rho_2 - \rho_1}{\rho_2 + \rho_1}k - \frac{\sigma}{\rho_2 + \rho_1}k^3. \qquad (1)$$

Here ρ_1 and ρ_2 are the densities of the lighter and heavier liquids, respectively, k is the wavenumber, g is the magnitude of the gravity acceleration, and σ is the surface tension coefficient. Thus, the instability develops faster if the density contrast is stronger, and the surface tension reduces the growth of the short-wave modes. This classical result was later verified in a number of experiments[7,8].

Later, Kurowski et al.[9] developed a theory of the Rayleigh-Taylor instability of a plane diffusion front, when in a single-phase liquid the field of the concentration of an added impurity experiences a strong transition

[a)] Electronic mail: A.Vorobev@soton.ac.uk

This manuscript was accepted by Phys. Fluids. Click here to see the version of record.

between two different levels (namely, the concentration profile was set by a similarity solution, $\sim \mathrm{erf}(z/\sqrt{Dt})$, where z is the coordinate perpendicular to the diffusion front, D is the diffusion coefficient, and t is the time). The linear stability theory was developed for a 'frozen' concentration profile, that is, in assumption that the spreading of the diffusion front occurs much slower than the growth of normal perturbations. For inviscid liquids, in the limit of the short wave perturbations (larger wavenumbers), the growth rate was found to be

$$\omega \simeq \frac{gR}{4Dk}, \tag{2}$$

where $R = \rho^{-1}\frac{d\rho}{dC}$ is the solutal expansion coefficient.

The development of the Rayleigh-Taylor instability is normally initiated by the exponential growth of several concurrent modes as determined by equations (1) or (2). When amplitudes of the unstable modes become significant compared with their wavelengths, the growth of such modes becomes slower, and at some stage, the modes with longer wavelengths ('bubbles') dominate the development of the instability, defining the spreading of the mixing zone that is formed at the liquid/liquid boundary. The thickness of the fully developed turbulent mixing layer grows as $\sim gt^2$. The turbulent regimes of the Rayleigh-Taylor instability of two miscible liquids (that were obtained by either two streams of the same liquid taken at different temperatures or by taking the mixture of brine and fresh water) were experimentally studied in Refs. 10–14. The phenomenological theories of the turbulent Rayleigh-Taylor instability of two miscible liquids were also developed (see e.g. Refs. 15 and 16).

The direct numerical simulation of the turbulent regimes of the Rayleigh-Taylor instability using the modelling approach similar to the one taken by Kurowski et al.[9], i.e. with no phases introduced, was developed in a number of works[17–21]. In particular, a strong dependence of the mixing dynamics on the initial conditions was reported,[17] which was later confirmed, and a favourable agreement of the results of the direct numerical simulations with the earlier experiments was achieved only when the initial conditions were carefully set.[20,21] It was found that the initial development of the instability exhibits a two-dimensional character, and the turbulence becomes three-dimensional at latter stages. The similarities and differences in the mixing dynamics in the $2D$ and $3D$ turbulent flows were also studied.[18] It was found that despite that the $3D$ mixing zone expanded twice faster, the overall development of the Rayleigh-Taylor instability occurred similarly in both cases. Payr et al.[19] studied the stability of the concentration front in a vertical capillary tube. The viscous effects, with the concentration-dependent viscosity were included into their model, which brought an unexpected complex dependence of the mixing rate on the interface thickness: it was shown that interfaces with the intermediate value of the interface thickness turned out to be more unstable than the thinner or thicker interfaces.

All earlier theoretical studies of the Rayleigh-Taylor instability of miscible liquids define the diffusion process using the classical Fick's law (the diffusion flux is proportional to the gradient of concentration), and, in addition, all earlier studies neglect the interfacial stresses.[9,17–21] It was however earlier noted by a number of researchers (see e.g. Refs. 22 and 23 for further references) that for an accurate description of an evolution of a heterogeneous binary mixture these two assumptions need to be reconsidered. Firstly, the interpretation of the experimentally-observed behaviour of slowly miscible interfaces requires the concept of the dynamic interfacial stresses (as the mixing usually occurs very slowly and the phases remain clearly distinguished for prolonged time periods; moreover, the inclusions are frequently of the spherical shape that can be explained by the surface tension effect, as e.g. one may observe during the process of dissolution of a honey droplet in tea). Secondly, the Fick's law is strictly valid only for the description of the diffusion of minor impurities, and, strictly speaking, this law is not applicable for sharper concentration gradients that are typical for the mixing of two liquids. In addition, the diffusion in a system of two liquids with different densities is complicated by the effect of barodiffusion.[24–27] The extended Fick's law, that defines the diffusion flux through the gradient of the chemical potential, takes these effects into account.

Korteweg[28] and van der Waals[29] proposed to model the interfacial stresses at a miscible boundary by using the concentration gradients. Zeldovich[30] and Cahn & Hilliard[31] proposed to re-define the free energy function for such a binary system by using the following expression,

$$f = f_0(C) + \frac{\epsilon}{2}\left(\nabla C\right)^2. \tag{3}$$

Thus, they proposed adding a new term that takes into account the additional interfacial energy associated with a miscible boundary. The role of this term is determined by a small capillary constant ϵ, so that this term is only important in the regions of large concentration gradients (that correspond to the regions of interface boundaries). The concentration in equation (3) is defined as the mass fraction of one of the components in a mixture.

Equation (3) forms the basis for the phase-field approach to be used for the modelling of heterogeneous binary mixtures. The full set of hydrodynamic equations, the so-called Cahn-Hilliard-Navier-Stokes equations, where derived by Lowengrub and Truskinovsky.[32] The full equations include the effect of quasi-compressibility, i.e. the dependence of the mixture density on concentration, which makes them difficult for numerical solution. In all publications, the reduced equations, written either for density-matched liquids or in the framework of the Boussinesq approximation of the full equations,[33–36] are used as a numerical tool capable of tracing the dynamics of immiscible interfaces. On the basis of this approach even some classical observations for the initial development of the Rayleigh-Taylor instability of immiscible interfaces were reproduced.[34–36]

In our work[37] we proposed to use the phase-field approach as a physics-based model for description of evolving miscible liquids, and we re-derived the Boussinesq approximation of the full Cahn-Hilliard-Navier-Stokes equations. The main difference in the resultant governing equations for the miscible liquids, in comparison with

ACCEPTED MANUSCRIPT

AIP Publishing

This manuscript was accepted by Phys. Fluids. Click here to see the version of record.

the model used in Refs. 34–36, is the additional term in the expression for the chemical potential that defines the effect of barodiffusion[24] (i.e. the diffusion flux driven by pressure gradients, namely, by hydrostatic and capillary pressure differences). For the mixing of two liquids, the barodiffusion term was found to have the same magnitude as the natural convective force in the Navier-Stokes equation, and thus it needs to be taken into account when the convective force is important. The other major difference of our study from the works[34–36] is that we study the equilibration of the binary mixture from an initial thermodynamically non-equilibrium state to the state of thermodynamic equilibrium. In works[34–36] the initial state corresponds to the state of thermodynamic equilibrium, which makes the diffusive mass transport negligible.

The new equations were applied for the investigation of the linear stability of miscible interfaces using the approximation of a 'frozen phase boundary'.[38] It was demonstrated that the eigenvalue spectra for a sharp immiscible interface could be successfully reproduced for long-wave disturbances, i.e. with the wavelengths much exceeding the interface thickness. It was found that the interfacial mass transfer introduces the additional dissipation, thus reducing the growth rate of the Rayleigh-Taylor instability. Moreover, the mutual actions of the diffusive and viscous effects could completely suppress the development of short wavelength perturbations. It was also found that the interfaces with the thickness exceeding a value that corresponds to the value of a thermodynamic equilibrium are thermodynamically unstable. In another work[39] we numerically investigate the enhancement of the liquid/liquid mixing by agitation of small gravity-capillary waves on the interface.

In the current work we aim to model the development of the Rayleigh-Taylor instability of a miscible interface using the full non-linear set of the equations that define the thermo- and hydrodynamic evolution of a heterogeneous binary mixture with the account of viscous, capillary and diffusive effects.

II. PROBLEM STATEMENT

We assume that two slowly miscible liquids are brought into contact, so that the denser liquid is placed on top of the lighter one. The liquids fill in a horizontal plain layer. The mixture is subject to the Rayleigh-Taylor instability, and the development of the hydrodynamic Rayleigh-Taylor instability is accompanied by bilateral diffusion across the liquid/liquid interface. The simultaneous hydrodynamic and thermodynamic evolution of the mixture turns the initial state into another state of hydrodynamic and thermodynamic equilibrium, and we study the transition between these two states. We assume that the hydrodynamic time scale is considerable shorter than the diffusion time scale, so a faster hydrodynamic evolution occurs on the background of slow diffusive transformations (this assumption is meant by the term 'slowly miscible liquids').

We present the results of the $2D$ direct numerical modelling of the Rayleigh-Taylor instability of a miscible interface. In particular, we study the stability of the liquid/liquid interface with respect to one-mode harmonic perturbation that is characterised by the wavenumber $k = 2\pi/\lambda$. The binary mixture is enclosed within a rectangular computational domain with the periodic boundary conditions in a horizontal direction. The vertical size of the computational domain is used as the length scale. The horizontal size of the domain is chosen to be equal to the wavelength, λ, of the initial perturbation, and thus it varies for different runs. The horizontal and vertical coordinates are denoted by x and y, respectively. The mixture is assumed to remain isothermal.

III. MATHEMATICAL MODEL

The phase-field approach is employed as a physics-based model capable of the accurate description of the thermo- and hydrodynamic evolution of a heterogeneous binary mixture (i.e. the mixture with interfaces). In this model, the concentration field is used to trace the evolution of the interfacial boundary, and the interface that separates two liquids is represented as a transitional layer of a finite thickness.

The specific free energy function for the binary mixture is defined by equation (3). The classical part of the free energy function, f_0, determines the possible thermodynamic states of the mixture and can be determined by the Landau formula,

$$f_0(C) = a(C - C_{cr})^2 + b(C - C_{cr})^4. \tag{4}$$

This expression would be particularly suitable to represent the equilibrium states of the binary mixtures with the so-called upper critical temperature (when the mixture is homogeneous in equilibrium above the critical temperature, and the mixture may be heterogeneous below the critical temperature), especially, the states of the mixture near the consolute point. We would further assume that the behaviour of a mixture with the upper consolute point is examined, and, for convenience, we shift the reference point for the concentration field as follows, $(C - C_{cr}) \to C$.

In the presence of the strong gravity-induced gradients in the field of concentration, or in the presence of strong hydrodynamic flows, expression (4) becomes less convenient, as in these cases the numerically calculated values of the concentration can become non-physical, taking the values outside of the range of concentrations that correspond to the pure components. In our papers[40–42] we found that the following expression,

$$f_0 = \left(a - \frac{3}{2}b\right) C^2 + \frac{3}{4}b\left(\frac{1}{2} + C\right)\ln\left(\frac{1}{2} + C\right) + \frac{3}{4}b\left(\frac{1}{2} - C\right)\ln\left(\frac{1}{2} - C\right), \tag{5}$$

is more convenient for numerical calculations. The latter equation represents the variation of a 'regular solution' function used by the theory of polymer solutions.[43] In the case of the symmetrical phase diagram and for the consolute point at $C = 0$ (or for the old reference point, at

ACCEPTED MANUSCRIPT

This manuscript was accepted by Phys. Fluids. Click here to see the version of record.

$C = \pm 1/2$), expression (5) coincides with the Landau formula in the vicinity of the consolute point. In addition, the logarithmic terms limit the field of concentration to the range $-1/2..1/2$ (or, in the old terms, to the range of 0..1). The free energy functions (4) and (5) are plotted in figure 1a, and figure 1b depicts the shapes of the phase diagrams, if one neglects the capillary and gravity effects.[44]

Expression (5) is used for the current work to define the classical part of the free energy function. The parameters a and b in this expression are treated as the two phenomenological coefficients with the values to be taken to provide a better matching with the experimental data. We however assume that b remains positive while a is either positive or negative depending on whether the binary system is single- or two-phase in equilibrium. Such expectations for a and b are natural for the system near the consolute point,[24] and we extend these expectations for other thermodynamic conditions.

The Boussinesq approximation of the full equations, derived in work[37], is used to define the isothermal evolution of the binary system:

$$\frac{\partial \vec{u}}{\partial t} + (\vec{u}\cdot\nabla)\vec{u} = -\nabla\Pi + \frac{1}{\mathrm{Re}}\nabla^2\vec{u} - C\nabla\mu, \qquad (6)$$

$$\frac{\partial C}{\partial t} + (\vec{u}\cdot\nabla)C = \frac{1}{\mathrm{Pe}}\nabla^2\mu, \qquad (7)$$

$$\nabla\cdot\vec{u} = 0, \qquad (8)$$

$$\mu = \mathrm{Gr}(\vec{r}\cdot\vec{\gamma}) + \mu_0 - \mathrm{Ca}\nabla^2 C, \qquad (9)$$

$$\mu_0 = \frac{df_0}{dC} = \frac{3}{4}\ln\left(\frac{1/2+C}{1/2-C}\right) - (3-2\mathrm{A})C. \qquad (10)$$

Here, $\vec{u}$ is the fluid velocity defined as the mass-averaged velocity for a two-phase fluid particle, Π is the modified pressure to be determined from the incompressibility constraint, and $\vec{\gamma} = -\vec{g}/g$ is the unit vector opposite to the vector of the gravity acceleration. These equations are applied to the whole multiphase system, including the interface. One sees that the Navier-Stokes equation contains an additional force (called the Korteweg force) that determines the interface morphology. The intensity of the diffusion process is defined by the generalised Fick's law, i.e. through the gradient of the chemical potential μ, which allows us to include, in addition to the usual diffusion driven by the concentration variations, the barodiffusion terms.[46]

The equations are written in the non-dimensional form and include the Grashof, Reynolds, Peclet, and capillary numbers,

$$\mathrm{Gr} = \phi\frac{gL_*}{\mu_*},\ \mathrm{Re} = \frac{\rho_*\mu_*^{1/2}L_*}{\eta_*}, \qquad (11)$$

$$\mathrm{Pe} = \frac{\rho_* L_*}{\alpha\mu_*^{1/2}},\ \mathrm{Ca} = \frac{\epsilon}{\mu_* L_*^2}. \qquad (12)$$

In these formulae L_* is the typical size, $\rho_* = \rho_1$ is used as the density scale, μ_* is the unit of the chemical potential, η_* is the viscosity scale, α is the mobility constant, and $\phi = (\rho_2 - \rho_1)/\rho_1$ is the density contrast (that is equal to twice the Atwood number). The typical scale of the velocity field is $\mu_*^{1/2}$.

It is necessary to note that the above definitions of the non-dimensional parameters are different from the standard definitions that would be given on the basis of the standard phenomenological parameters, such as the surface tension and diffusion coefficients. We keep using the conventional names and notations, as these non-dimensional parameters appear in front of the corresponding terms of the hydrodynamic equations. The only exception is the capillary number, Ca, which definition (11) is completely different from the classical definition of the capillary number. The parameter used in the current work is directly proportional to the capillary constant and thus it determines the importance of the capillary effects. In some works (e.g. Ref. 35) the same parameter is called the Cahn number.

The parameter $\mathrm{A} = a/b$ comes from the equation for the free energy function (5), and this parameter determines the thermodynamic states of the mixture. Essentially, this parameter sets the temperature of the binary mixture, and whether this temperature is above ($A > 0$) or below ($A < 0$) the critical value. All calculations in the current work are carried out for a fixed value $A = -1/2$.[47]

The governing equations (6)-(10) were derived for two liquids with different viscosity coefficients. For the multiple-scale analysis of the equations, the difference in the viscosity coefficients was assumed to be of the same order as the difference in densities that is small for all liquid/liquid binary mixtures. One single Reynolds number is sufficient in this case, as the terms in the governing equations that characterise the differences in the viscosity would be too small. When the viscosity difference is not small, the governing equations need to be reconsidered, and this has not been done in the present work.

It can be shown that the surface tension coefficient associated with the flat phase boundary between two semi-infinite liquid continua is

$$\sigma_\infty = \mathrm{Ca}\int_{-\infty}^{\infty}\left(\frac{\mathrm{d}C}{\mathrm{d}z}\right)^2\mathrm{d}z, \qquad (13)$$

where z is the coordinate across the interface. For an equilibrium interface and with no gravity effect, the interface thickness can be evaluated as $\delta_{eq} = \sqrt{-\mathrm{Ca}/\mathrm{A}}$ and the surface tension coefficient as $\sigma_\infty = \frac{1}{3}\sqrt{-\mathrm{CaA}}$.[32,38]

The governing equations (6) are supplemented with the periodic boundary conditions in the horizontal direction, and with the following conditions at the bottom and upper plates,

$$y = 0, 1:\ u_x = u_y = 0,\ \frac{\partial C}{\partial y} = 0,\ \frac{\partial \mu}{\partial y} = 0. \qquad (14)$$

Thus, the no-slip boundary conditions are used for the velocity field. For the chemical potential, we impose the absence of the diffusive flux through the plates. The conditions for the concentration reflect the wetting properties of the walls. We however consider the simplest case when the molecules of the mixture components interact with the wall equally, so the contact angle is set to be 90^0.

At the start of a numerical run the binary mixture is assumed to be at rest ($\vec{u} = 0$), and the shape and position of the interface is set by the following concentration

ACCEPTED MANUSCRIPT

This manuscript was accepted by Phys. Fluids. Click here to see the version of record.

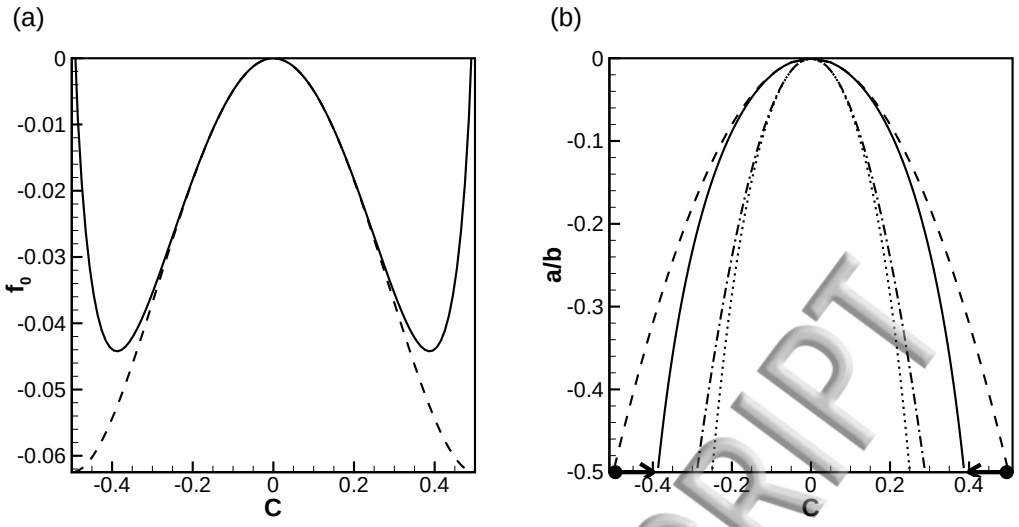

FIG. 1. (a) The free energy function and (b) the phase diagram determined by expressions (4), dashed lines, and (5), solid lines. The phase diagram is shown for the case of neglected capillary and gravity effects. The phase diagram is defined by the coexistence or binodal curves that depict the states of thermodynamic equilibrium when two phases co-exist with no mass transfer across the interface. If concentrations in the neighbouring phases are different from the ones determined by the coexistence curve then the mixture is thermodynamically unstable with non-zero mass transfer across the interface. In addition, the dashed-dotted and dotted lines in (b) show the boundaries of the region of spinodal decomposition (for expressions (4) and (5), respectively), that define the zones of absolute instability of matter.[45] Two points in (b) show the initial concentrations in the phases, and the arrows indicate the direction of the studied evolution of the binary system.

profile,

$$C_0(x,y) = 0.495 \tanh\left(\frac{y - 0.5(1 + 0.1\cos(kx))}{\delta_0}\right). \quad (15)$$

Here ± 0.495 are the initial concentrations in the two liquids in contact, and δ_0 is the initial interface thickness. Since the initial state of the binary mixture is different from the state of thermodynamic equilibrium, the initial interface thickness δ_0 is different from its equilibrium value δ_{eq}. This is one of the differences of the current work from other similar studies[34–36], where the phase-field method is used for modelling the evolution of a binary system that experiences some hydrodynamic changes, but it is assumed that the system always resides in a state of thermodynamic equilibrium (i.e. $\delta_0 = \delta_{eq}$). We use the phase-field model as a physics-based model for the miscible heterogeneous system, the model that is capable of tracing the transformations of the interface shape and the interfacial diffusion through the interface.

In addition, it is necessary to note that on a macroscopic scale the interface between two liquids is infinitely sharp, and the limiting behaviour for $\delta \to 0$ is of the primary interest for the phase-field approach.

IV. NUMERICAL SOLUTION. CONVERGENCE

For the numerical solution, the equations are rewritten into the streamfunction-vorticity formulation, and the resultant equations are solved using the finite-difference method on a uniform mesh. The explicit first order in time and second-order in space discretisation scheme is used.

Various integral characteristics of the binary system are calculated on the bases of the concentration and velocity fields.

1. We calculate the total kinetic energy of the fluid motion as defined by equation,

$$E_k = \frac{1}{2}\int_V u^2 \mathrm{d}V. \quad (16)$$

Here V is the volume of the computational domain.

2. We calculate the volume of the transition layer that separates the liquids, V_δ, summing up the volumes of all cells for which $|C| < 0.2$.

3. We calculate the length, L, and the thickness, δ, of the interfacial layer. The position of the interface is determined by the concentration level $C = 0$. To determine the length of the interface, L, we first search for the nodes between which the concentration changes its sign, and determine the position of the interface between these nodes by using the linear interpolation; we next obtain the length of an interface element that lies within a cell made of four nodes; and finally we sum up these elementary lengths to obtain the length of the whole interfacial line. Finally, the thickness of the interface layer is determined as $\delta = V_\delta / L$ (for 2D calculations, the surface area of the interfacial boundary is replaced by the interface length).

4. We calculate the coefficient of the surface tension as

$$\sigma = \frac{\mathrm{Ca}}{L}\int_V \left(\left(\frac{\partial C}{\partial x}\right)^2 + \left(\frac{\partial C}{\partial y}\right)^2\right)\mathrm{d}V. \quad (17)$$

ACCEPTED MANUSCRIPT

This manuscript was accepted by Phys. Fluids. Click here to see the version of record.

We calculate the average concentrations in each phase, as

$$C_{1,2} = \frac{1}{V_{1,2}} \int_{V_{1,2}} C \mathrm{d}V, \tag{18}$$

where V_1 and V_2 are the volumes of the first and second phases, respectively, which are in fact the same, $V_1 = V_2 = V/2$, due to symmetry of the problem.[48]

To choose the optimal numerical resolution we performed the set of numerical runs using the numerical grids with the different numbers of the nodes. The results of the runs are depicted in figure 2, where we plot the time dependencies of the total kinetic energy of the hydrodynamic motion induced in the computational domain and the interface length for two different levels of the Peclet numbers, $Pe = 10^5$ (figure 2a) and $Pe = 10^7$ (figure 2b). In both figures one can clearly see the convergence of the curves to some limiting results. The convergence of the results is achieved much faster (i.e. with much lower numerical resolution) at the lower Peclet number, $Pe = 10^5$, which seemingly needs to be explained by much thinner diffusive length scales that characterise the problem at higher Peclet numbers. On the basis of this analysis the grid of 500×500 nodes was chosen for the runs with $Pe = 10^5$ and the grid of 1440×1440 nodes was chosen for the run with $Pe = 10^7$.

V. RESULTS

Figure 3 depicts the fields of the concentration and velocity at different time moments showing the stages of the time evolution of the binary mixture. At the initial moment the sharp interface separates the liquids, with the heavier liquid on the top. The shape of the interface is slightly curved as set by the initial concentration profile (15). The initial flow velocity is set to be zero. The configuration is gravitationally unstable that leads to the development of the Rayleigh-Taylor instability, i.e. to the growth of the interface deformation accompanied by the hydrodynamic flow. At some point the heavier liquid blob reaches the bottom wall, ultimately, overturning the mixture components so the heavier liquid starts to occupy the lower half of the layer. The re-arrangement of the binary mixture (especially, at its initial stages) is accompanied by the hydrodynamic motion. In the end of this reconfiguration only some smaller droplets of the heavier liquid remain attached to the upper wall, and some droplets of the lighter liquid remain attached to the bottom. The sizes of the droplets very slowly decrease due to the dissolution process that is driven by diffusion.

The evolution of the mixture enclosed in a plane layer is examined, and this strongly limits the development of the Rayleigh-Taylor instability, for instance, restricting the maximum values of the flow velocity and the interface length, and the overall time of the hydrodynamic evolution. Owing to this restriction the turbulent stages of the Rayleigh-Taylor instability are never reached in our calculations. In addition, the development of a single initial perturbation, with the wavelength always comparable to the height of the layer, is only traced. We do not observe the concurrence or selection of the unstable modes, which would be typical for the natural development of the instability.

Figure 4 depicts the snapshots of the chemical potential. The initial levels of the chemical potential in the components of the binary mixture are different (that corresponds to the thermodynamically non-equilibrium state), with a sharp jump across the interface. In the final equilibrium state the binary system is characterised by the uniform field of the chemical potential, $\mu = 0$. Since the gradient of the chemical potential determines the magnitude of the diffusive flux, one may easily conclude that the diffusion is more intensive at the point of the first contact of two liquids, and the intensity of the diffusion is strongly reduced at the later time moments.

Figure 5 depicts the time evolutions of these integral characteristics. The development of the Rayleigh-Taylor instability can be traced through the total kinetic energy of the hydrodynamic motion induced in the layer, and this is shown in figure 5a, and through the deformation of the interface determined by its length, the time changes of this quantity are shown in figure 5b. One can notice that at the initial stage the values of these characteristics grow very rapidly, which is in agreement with the assumptions of the linear theory. Surprising results are that the development of the instability at the lower Peclet numbers (i.e., for the stronger interfacial diffusion) occurs faster, and the maximum value of the kinetic energy achieved in this case is also greater. The linear growth of the instability is observed until the first peak in the lines of the kinetic energy is reached, i.e. until the time moments $t \sim 20$ at $Pe = 10^5$ and $t \sim 50$ at $Pe = 10^7$ (these time moments can be clearly seen in figure 2). The curves of the kinetic energy in figure 5a also show the second peaks when some weaker hydrodynamic flows are induced by the oscillation (at $\mathrm{Pe} = 10^5$) or even detachment (at $\mathrm{Pe} = 10^7$) of the central droplets that are seen in figures 3e,f.

In figure 5b one can see that the length of the interface increases in time due to deformation of the interface surface. The interface has the maximum length at the time moment that corresponds to figure 3d. The rupture of the interface and the rearrangement of the phases that occur at the following time moment results in a sharp drop of the value of the interface length. At the end of the numerical runs the interface lengths do not equal to the initial value due to the small droplets that remain attached to the top and bottom walls.

Figure 5c shows the time variations of the interface thickness. For the calculations shown in figure 5 the initially set value of the interface thickness is 1.5-times lower than the equilibrium value, $\delta_{eq} = \sqrt{-Ca/A}$. Owing to the process of the interfacial diffusion, the interface smears in time, ultimately, reaching its equilibrium value. For comparison, in these figures we also show the curves for the pure diffusion runs, when the mixture components were assumed to have the matched densities, and thus no hydrodynamic motion is induced in the system. The purely diffusive evolution of the system predictably occurs much slower.

ACCEPTED MANUSCRIPT

This manuscript was accepted by Phys. Fluids. Click here to see the version of record.

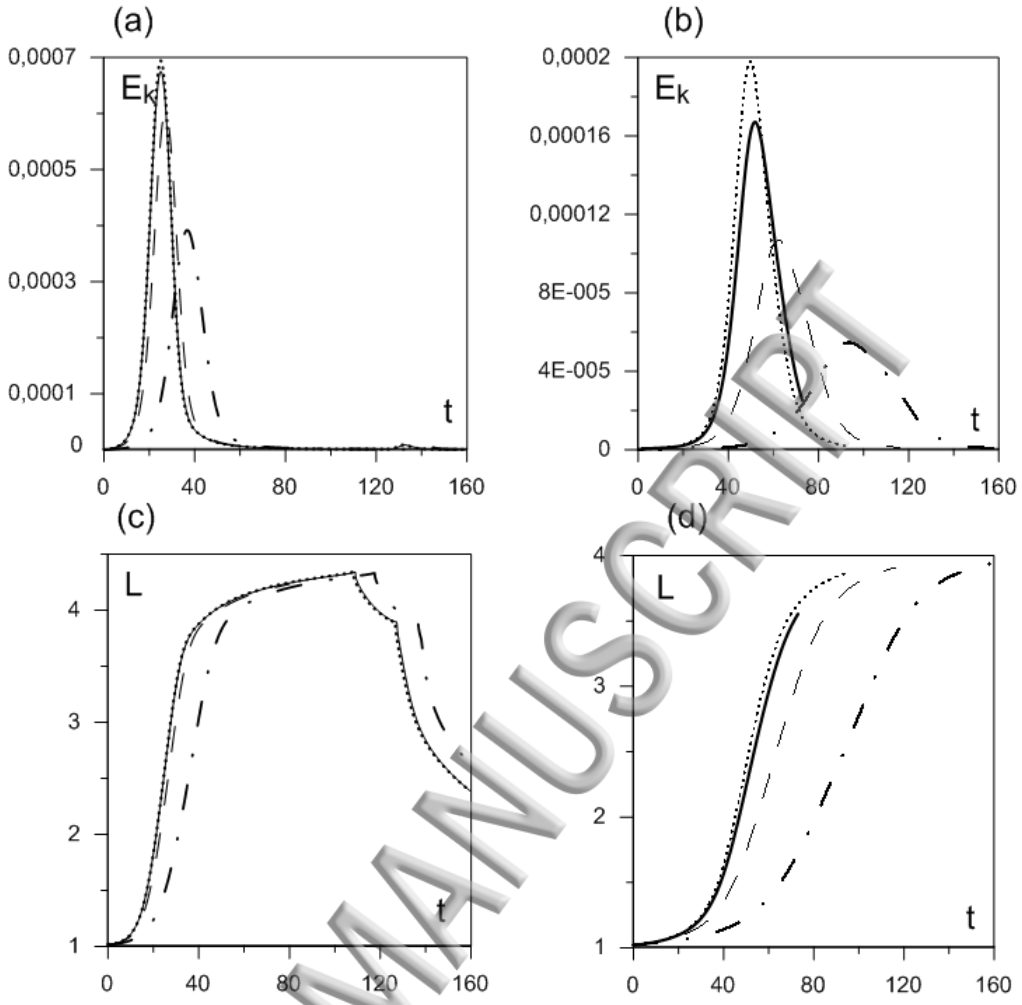

FIG. 2. The curves of the total kinetic energy (a,b) and the interface length (c,d) vs. time are plotted for the numerical runs fulfilled with the use of the different numerical grids: (a) $Pe = 10^5$, and 250×250 (dash-dotted line), 360×360 (dashed line), 500×500 (solid line), 750×750 (dotted line); (b) $Pe = 10^7$, 800×800 (dash-dotted line), 1024×1024 (dashed line), 1280×1280 (solid line), and 1440×1440 (dotted line). The other parameters for the runs were $\delta_0 = 5.96 \cdot 10^{-3}$, A $= -0.5$, Ca $= 4 \cdot 10^{-5}$, Gr $= 0.1$, Re $= 100$, and $k = 2\pi$.

To our surprise, the time evolution of the interface thickness is more complex than just the simple diffusion smearing. At the initial time period the interface thickness does not increase as one expects, and even, on opposite, the thickness of the interface decreases, and the amplitude of this decrease is greater than the expected change due to the diffusive growth, $|\delta_{eq} - \delta_0|$. It seems that the stretching (or elongation) of the interface layer due to its deformation results in the interface thinning, similar to the thinning of elastic materials (e.g. an elastic membrane) upon their tensile deformations. This effect is completely disregarded in the linear stability theories,[9,38] and this should be one of the major weaknesses of such theories.[49]

One can also notice that the initial change of the interface thickness is weaker for the lower Peclet number, which indicates that the changes of the interface thickness are determined by the interplay of two effects, the interface thinning due to stretching and the interface smearing due to diffusion. At lower Peclet numbers the effect of diffusion is stronger, and this partially counteracts the effect of the interface stretching, restricting the increase in the values of the surface tension coefficient.

Figure 5d shows the time evolution of the surface tension coefficient. In general, this quantity is reciprocal to the thickness of the interface (e.g. for the interface with the profile approximated by the tanh-function, the value of the surface tension coefficient and the interface thickness are related as $\sigma_\infty = \mathrm{Ca}/(3\delta)$, see e.g. Ref. 38), and understanding of this could be used to explain the obtained dependencies. On the longer time scales, the value of the surface tension coefficient decreases due to diffusive smearing of the interface, although, at the initial time period the surface tension coefficient experiences a very strong growth due to the interface thinning that is forced by the interface stretching (elongation).

Figure 5e depicts the time variations of the volume of the transitional layer that separates the liquids, which generally follow the curves of the interface length, indicating that amplitude of the increase of the interface length is greater than the amplitude of the increase of the interface thickness (since $V_\delta = L\delta$).

ACCEPTED MANUSCRIPT

This manuscript was accepted by Phys. Fluids. Click here to see the version of record.

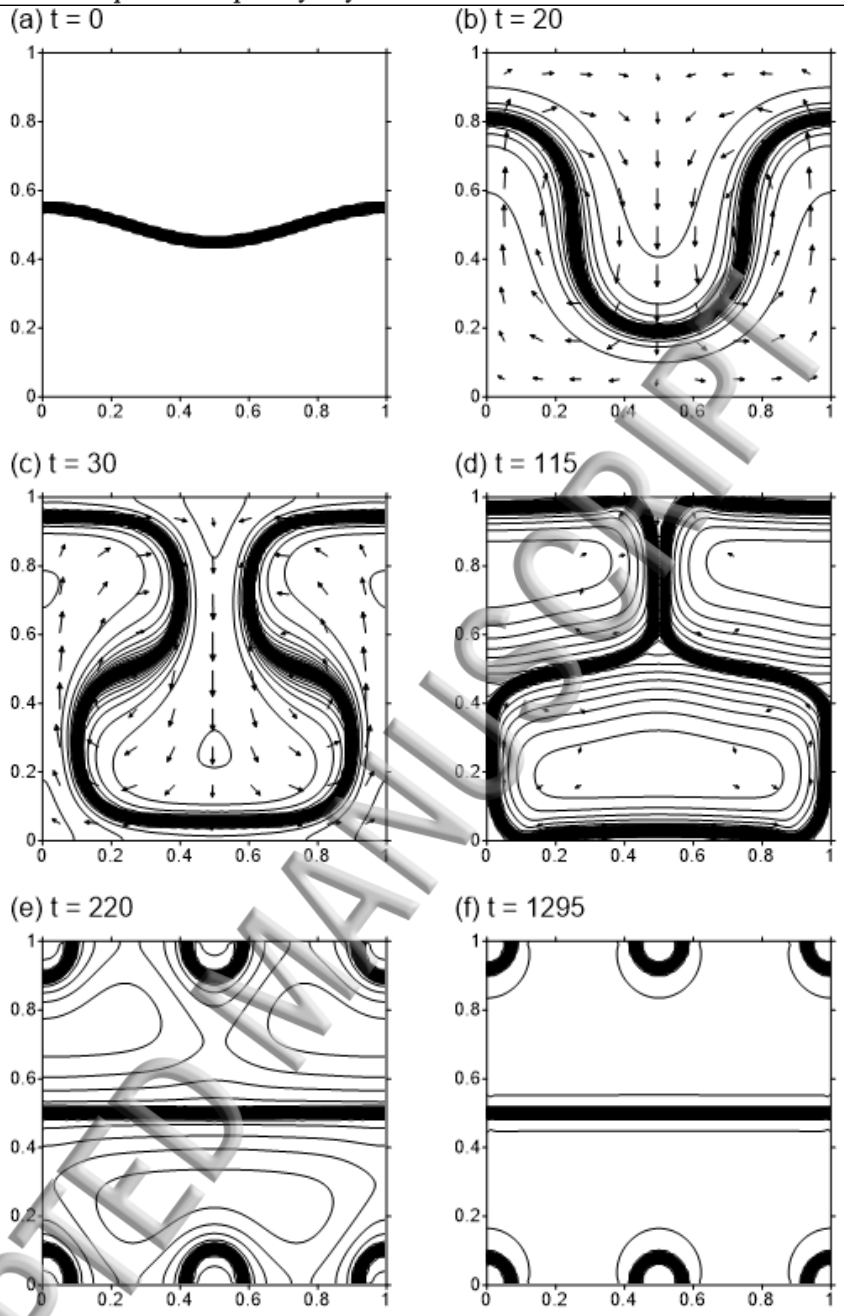

FIG. 3. The fields of concentration (depicted by isolines) and velocity (depicted by arrows) are shown for the different time moments. The data are obtained for $\delta_0 = 5.96 \cdot 10^{-3}$, A $= -0.5$, Ca $= 4 \cdot 10^{-5}$, Gr $= 0.1$, Re $= 100$, Pe $= 10^5$. The horizontal size of the computational domain equals to the wavelength of the initial perturbation, i.e. $\lambda = 1$, and hence the wavenumber for this calculation is $k = 2\pi$. The levels of the concentration vary in the range of $-0.5..0.5$ with the step of 0.01. The arrow lengths reflect the magnitude of the velocity.

Figure 5f shows the average concentration in one of the liquids (the average concentration in another liquid is exactly the same, with values that can be obtained by the sign change). The levels of the average concentration change from the initial values, $\pm 1/2$, to their equilibrium (saturation) values, which are approximately ± 0.388 for the chemical potential defined by the free energy function (5). For $Pe = 10^5$, the equilibrium state is reached at $t \approx 1500$, while for the pure diffusive run, i.e. with the omission of the hydrodynamic effects, the equilibrium state is reached at $t \approx 6000$.

A surprising enhancement of the molecular-level mixing of the liquids that is revealed in figure 5f through the quick jumps in the values of the average concentrations in each phase should be explained by the interface stretching that characterises the initial stages of the mixture evolution and that leads to a substantial enlargement of the contact area between the phases. For comparison, figure 10f also shows the average concentration for a density-matched pair of liquids, when the Rayleigh-Taylor instability does not develop, and the interface remains flat. Since the hydrodynamic processes cease to

ACCEPTED MANUSCRIPT

This manuscript was accepted by Phys. Fluids. Click here to see the version of record.

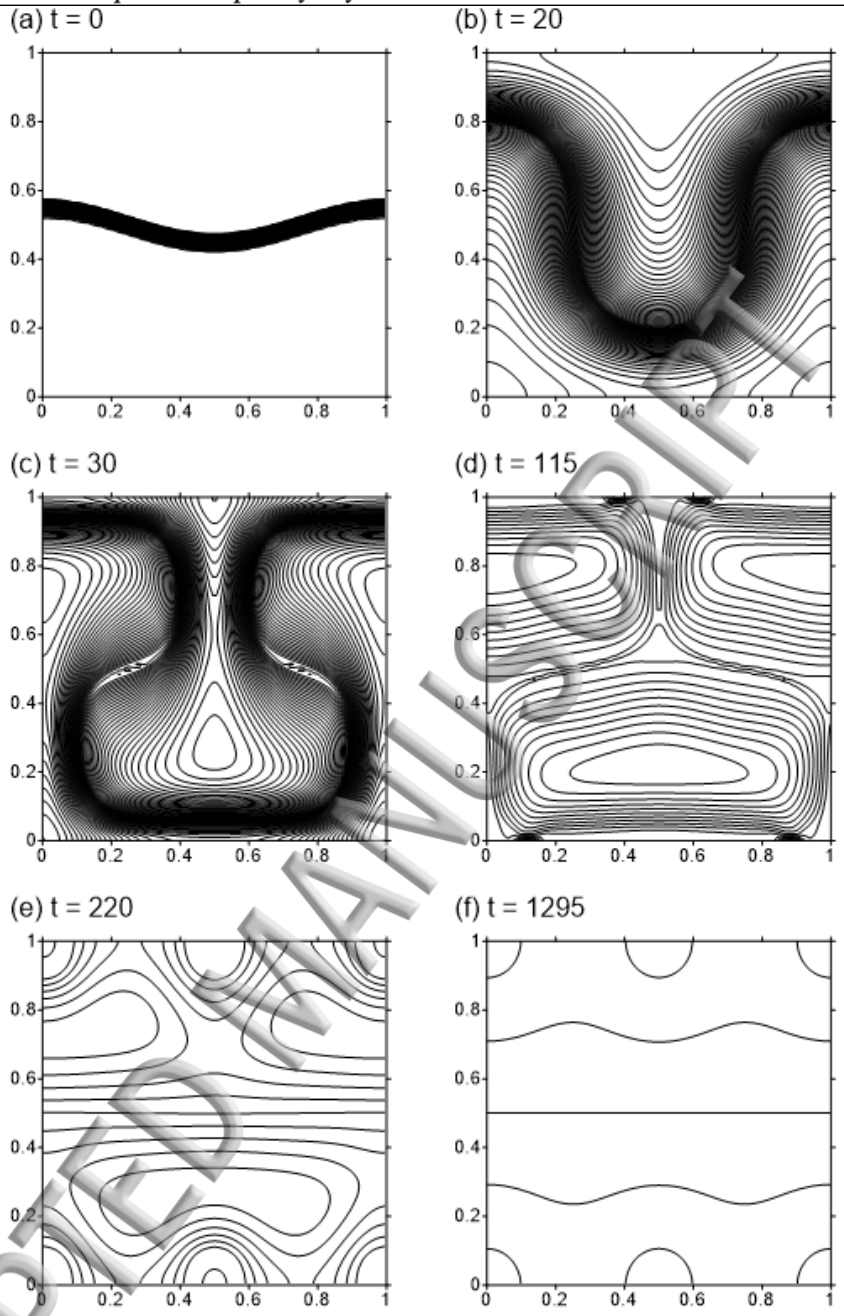

FIG. 4. The fields of chemical potential are shown for the different time moments. The data are obtained for $\delta_0 = 5.96 \cdot 10^{-3}$, $A = -0.5$, $Ca = 4 \cdot 10^{-5}$, $Gr = 0.1$, $Re = 100$, $Pe = 10^5$, and $k = 2\pi$. The shown levels of the chemical potential vary in the range $-1.9..1.9$ with the step of 0.05.

exist at about $t \approx 100$, when the mixture components are already overturned but the state of thermodynamic equilibrium is still not reached, the role of diffusion remains pivotal, so that the complete thermodynamic equilibration of the system occurs substantially longer for the runs with higher Peclet numbers. One can also notice that since the hydrodynamic processes become virtually non-existent at $t \approx 100$, then, starting from this moment, the calculations could be simplified by neglecting the convective terms in the governing equations.

Thus, the variations of the interfacial thickness and the average concentration are generally expected to be determined by the slow diffusion process, so that they should remain nearly constant over a short period of time. We however found that both quantities experience the fast time variations driven by the hydrodynamics. In figures 6 and 7 we show the initial time variations of the interface thickness and average concentration for the different values of non-dimensional parameters. One sees that at lower Peclet numbers (for more intensive diffusion) the smearing of the interfacial boundary is more pronounced (there is a stronger change in the values of the average concentration) and the effect of the interface stretching becomes less important. The runs fulfilled for higher Reynolds numbers reveal that both the rates of changes and the amplitudes of changes of interface thick-

ACCEPTED MANUSCRIPT

This manuscript was accepted by Phys. Fluids. Click here to see the version of record.

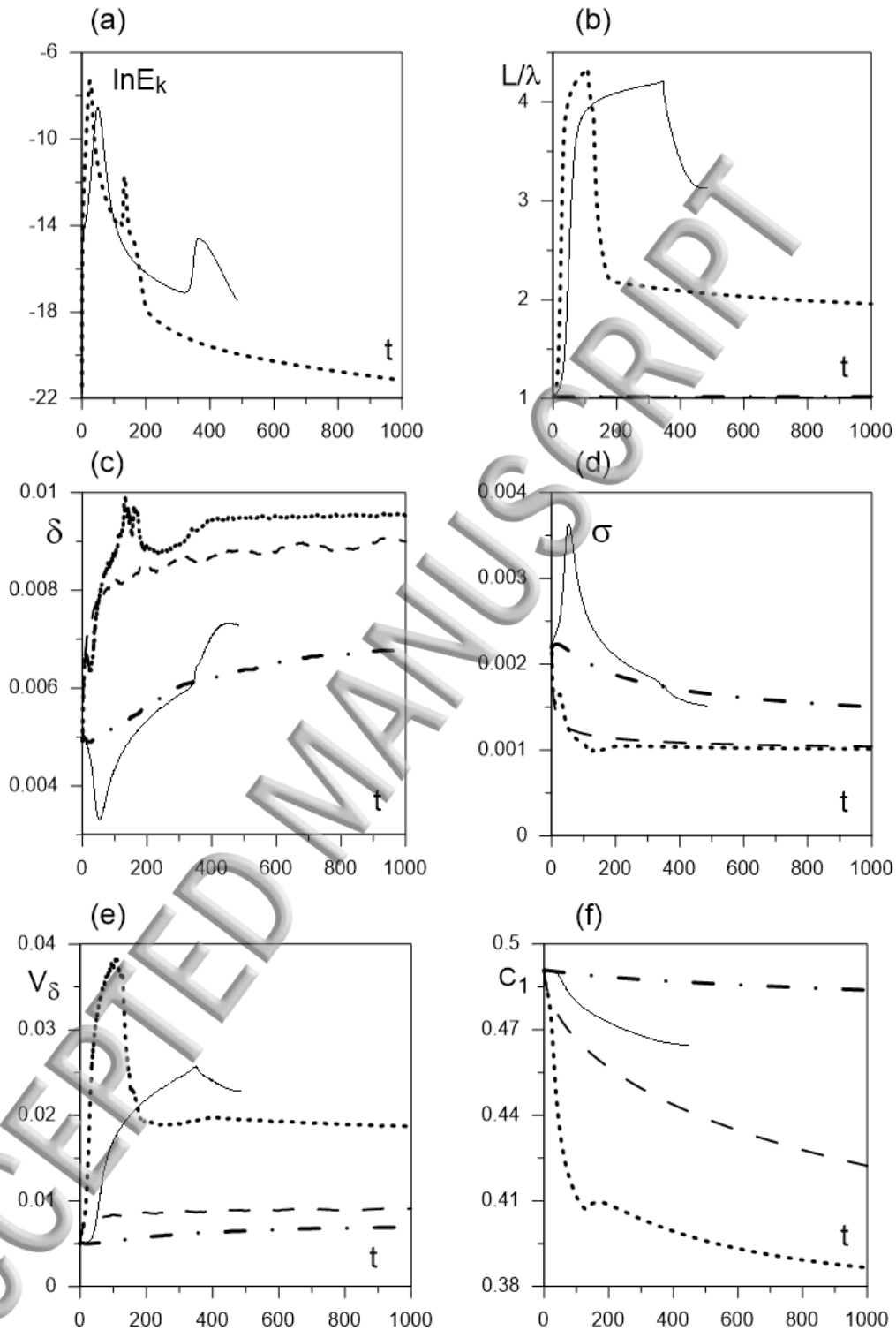

ACCEPTED MANUSCRIPT

FIG. 5. (a) The logarithm of the total kinetic energy vs. time; (b) the length of the interface scaled by the wavelength of the initial perturbation, L/λ, vs. time; (c) the thickness of the interface vs. time; (d) the surface tension coefficient vs. time; and (e) the volume of the transition layer vs. time, (f) the average concentrations in one phase vs. time (the average concentration in another phase $C_2 = -C_1$). The data are obtained for $k = 2\pi$, $\delta_0 = 5.96 \cdot 10^{-3}$, A $= -0.5$, Ca $= 4 \cdot 10^{-5}$, Gr $= 0.1$, Re $= 100$, and two different Peclet numbers, Pe $= 10^7$ (solid lines) and Pe $= 10^5$ (dotted lines). The two additional lines depict the results for the purely diffusion runs: the long-dashed line for Pe $= 10^5$ and the long-dash-dotted line for Pe $= 10^7$.

This manuscript was accepted by Phys. Fluids. Click here to see the version of record.

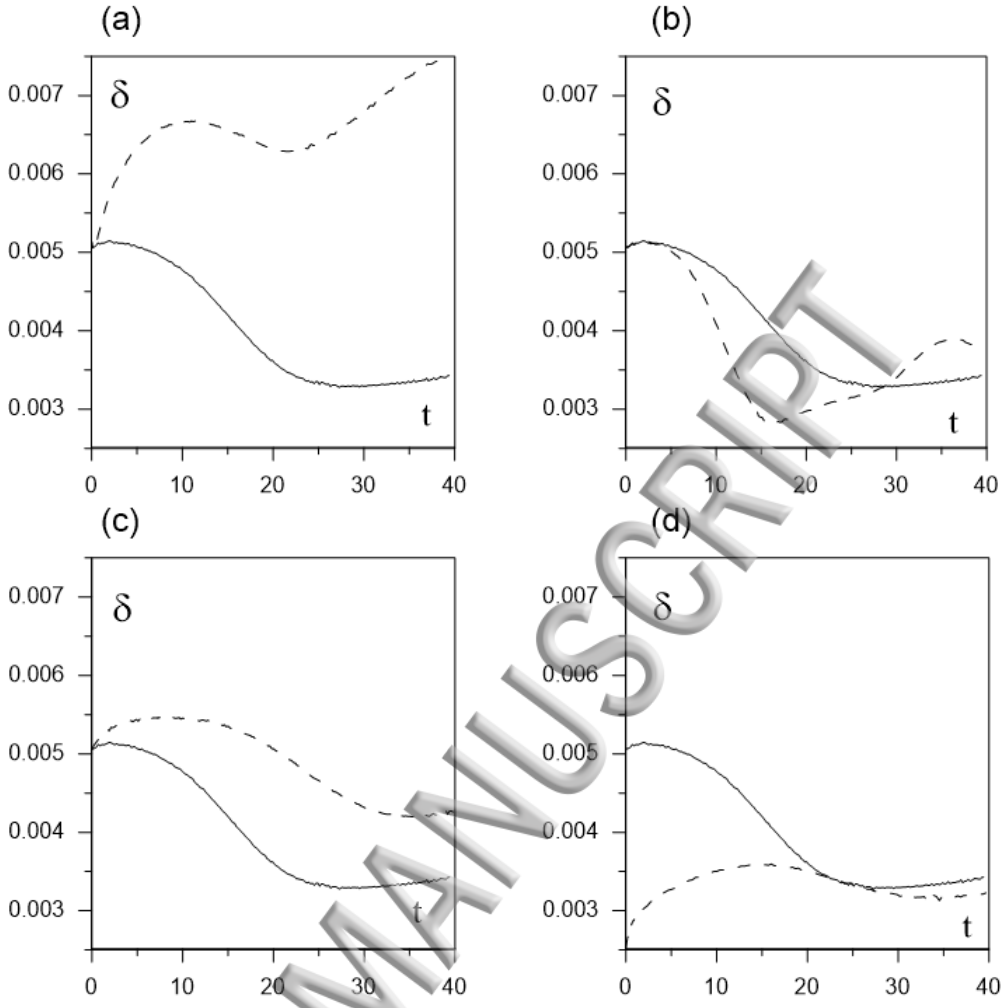

FIG. 6. The interface thickness vs. time. The plots are shown for (a) two different Peclet numbers (Pe = 10^5, dashed line, and Pe = 10^7, solid line), (b) two different Reynolds number (Re = 1200, dashed line, Re = 100, solid line), (c) two different capillary numbers (Ca = $8 \cdot 10^{-5}$, dashed line, Ca = $4 \cdot 10^{-5}$, solid line), and (d) two different initial thicknesses of the interfacial boundary ($\delta_0 = 2.98 \cdot 10^{-3}$, dashed line, and $\delta_0 = 5.96 \cdot 10^{-3}$ solid line). The default parameters are $k = 3.93$, $\delta_0 = 5.96 \cdot 10^{-3}$, A = -0.5, Ca = $4 \cdot 10^{-5}$, Gr = 0.1, Pe = 10^7, Re = 100, and one of these parameters was varied as defined above.

ACCEPTED MANUSCRIPT

ness and average concentration are even greater when viscous forces are lower. The increase in the capillary number slows down the development of the Rayleigh-Taylor instability, making the variations in the interface thickness smaller. The reduction of the initial interface thickness also leads to the smaller changes of the interface thickness, indicating that the effect of the interface thinning is likely to disappear in the limit of an infinitely sharp boundary (thus providing the transition of the current results to the classically-expected behaviour). Nevertheless, the changes of the average concentration remain at the same level when either the capillary parameter or the initial value of the interface thickness is varied.

Figure 8 depicts the time evolutions of some of the integral characteristics (for the run with $Pe = 10^5$) at the initial time period. To characterise the rate of the time changes we calculate the growth rate, ω, using the linear parts of the curves that depict the logarithm of the kinetic energy (figure 8b). Since every run is started with the non-zero deformation of the interface and with zero hydrodynamic flow, which is not an exact solution of equations (6), the curves of the kinetic energy demonstrate the short adjustment periods. But after that, the total kinetic energy (and all other quantities) grows exponentially until at least the time moment $t \sim 20$, that corresponds to the peak value of the kinetic energy. The growth rate that characterises the linear development of the Rayleigh-Taylor instability obviously depends on the shape of the initial deformation of the interface (that is determined by the wavenumber, k), and on the values of the other governing parameters. These dependencies are illustrated in figure 9.

In particular, figure 9a illustrates that the stronger gravity effect (i.e. the stronger density contrast between the components of the mixture) results in the faster development of the Rayleigh-Taylor instability. Figure 9b shows the role of the viscous effects on the development of the interface deformation. The lower Reynolds numbers correspond to the slower growth rates due the additional viscous damping. Figure 9c illustrates the action of the capillary effects. The stronger capillary forces reduce the growth rates of the Rayleigh-Taylor instability

AIP Publishing

This manuscript was accepted by Phys. Fluids. Click here to see the version of record.

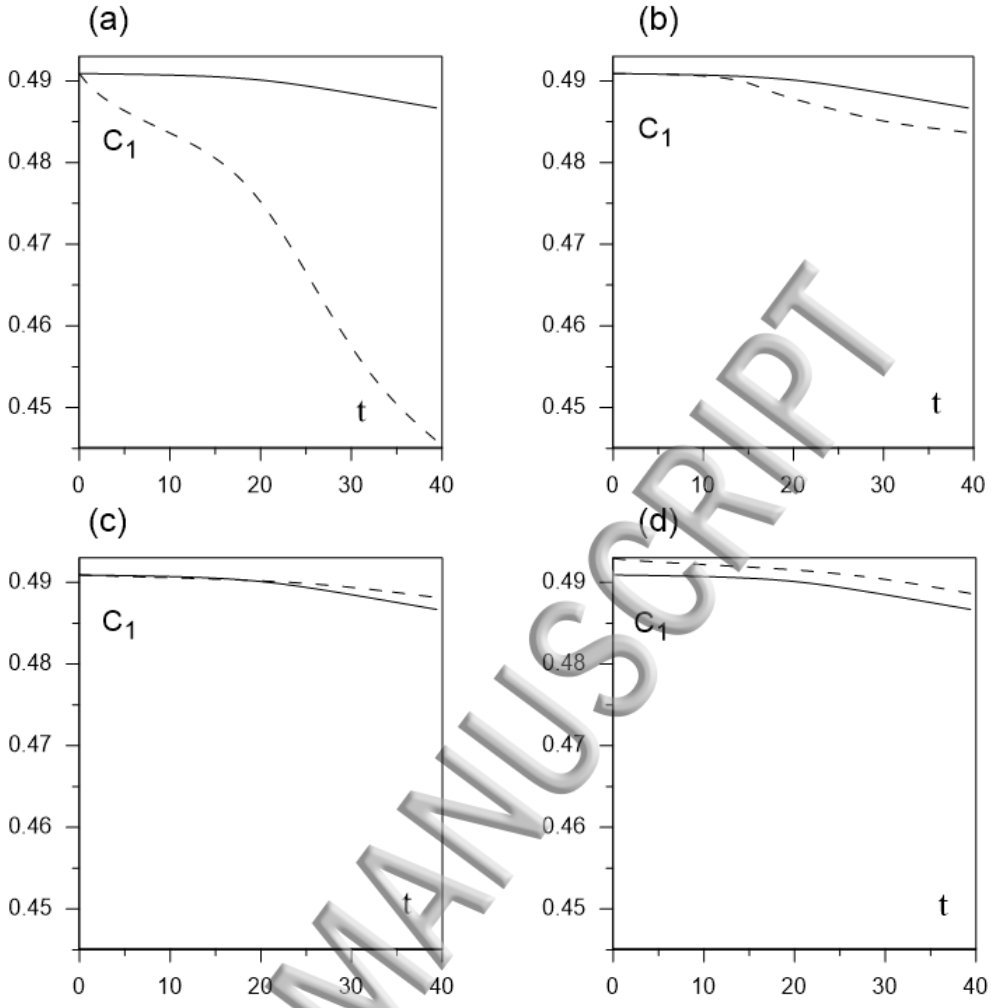

FIG. 7. The average concentration in one of the liquids, C_1, (the average concentration in the other liquid, $C_2 = -C_1$) vs. time. The curves are plotted for (a) two different Peclet numbers ($Pe = 10^5$, dashed line, and $Pe = 10^7$, solid line), (b) two different Reynolds number ($Re = 1200$, dashed line, $Re = 100$, solid line), (c) two different capillary numbers ($Ca = 8 \cdot 10^{-5}$, dashed line, $Ca = 4 \cdot 10^{-5}$, solid line), and (d) two different initial thicknesses of the interfacial boundary ($\delta_0 = 2.98 \cdot 10^{-3}$, dashed line, and $\delta_0 = 5.96 \cdot 10^{-3}$ solid line). The default parameters are $k = 3.93$, $\delta_0 = 5.96 \cdot 10^{-3}$, A $= -0.5$, Ca $= 4 \cdot 10^{-5}$, Gr $= 0.1$, Pe $= 10^7$, Re $= 100$, and one of these parameters was varied as defined above.

ACCEPTED MANUSCRIPT

and also limit the growth of the modes with the shorter wavelengths. All these predictions are in good agreement with the general expectations for the Rayleigh-Taylor instability and with the earlier predictions obtained on the basis of the linear stability theory.[38]

Figure 9d illustrates that the diffusion makes a contribution to the development of the Rayleigh-Taylor instability even on a shorter time scale (which was already seen in figure 5a). However, the dependencies of the growth rate on the Peclet number differ from those that were earlier derived on the basis of the linear stability theory. It was earlier concluded that the diffusion introduces the additional dissipation mechanism, just slowing down the development of the instability.[38] The opposite behaviour is depicted in figure 9d, with the growth rates being stronger at lower Peclet numbers (i.e. at stronger diffusion levels). The new result may be explained by the action of capillary effects that are determined by the surface tension coefficient. As noted above at higher Peclet numbers, the effect of diffusion is weaker, and the interface stretching results in much stronger capillary forces (see figure 5d). As a result, the runs with the higher Peclet number are characterised with the higher surface tension coefficients, and hence, with the lower growth rates for the Rayleigh-Taylor instability. This capillary damping also explains the surprising result depicted in figure 5a when at higher Peclet numbers the kinetic energy has a lower peak that is reached at a later time moment.

In figure 10 we demonstrate that the limit of inviscid fluids can be retrieved at $Re \sim 2000$. We also show that although at higher Peclet numbers the curves approach the lines that are obtained on the basis of the classical formula (here this formula is written in the non-dimensional form using the scales accepted in this work)[38,50]

$$-\frac{q(q+k)(q^2-k^2)}{\mathrm{Re}^2} = \frac{1}{2}\mathrm{Gr}k + \frac{\sigma}{2}, \qquad q \equiv \sqrt{k^2 - i\omega Re}. \tag{19}$$

that sets the values of the growth rates of the Rayleigh-

This manuscript was accepted by Phys. Fluids. Click here to see the version of record.

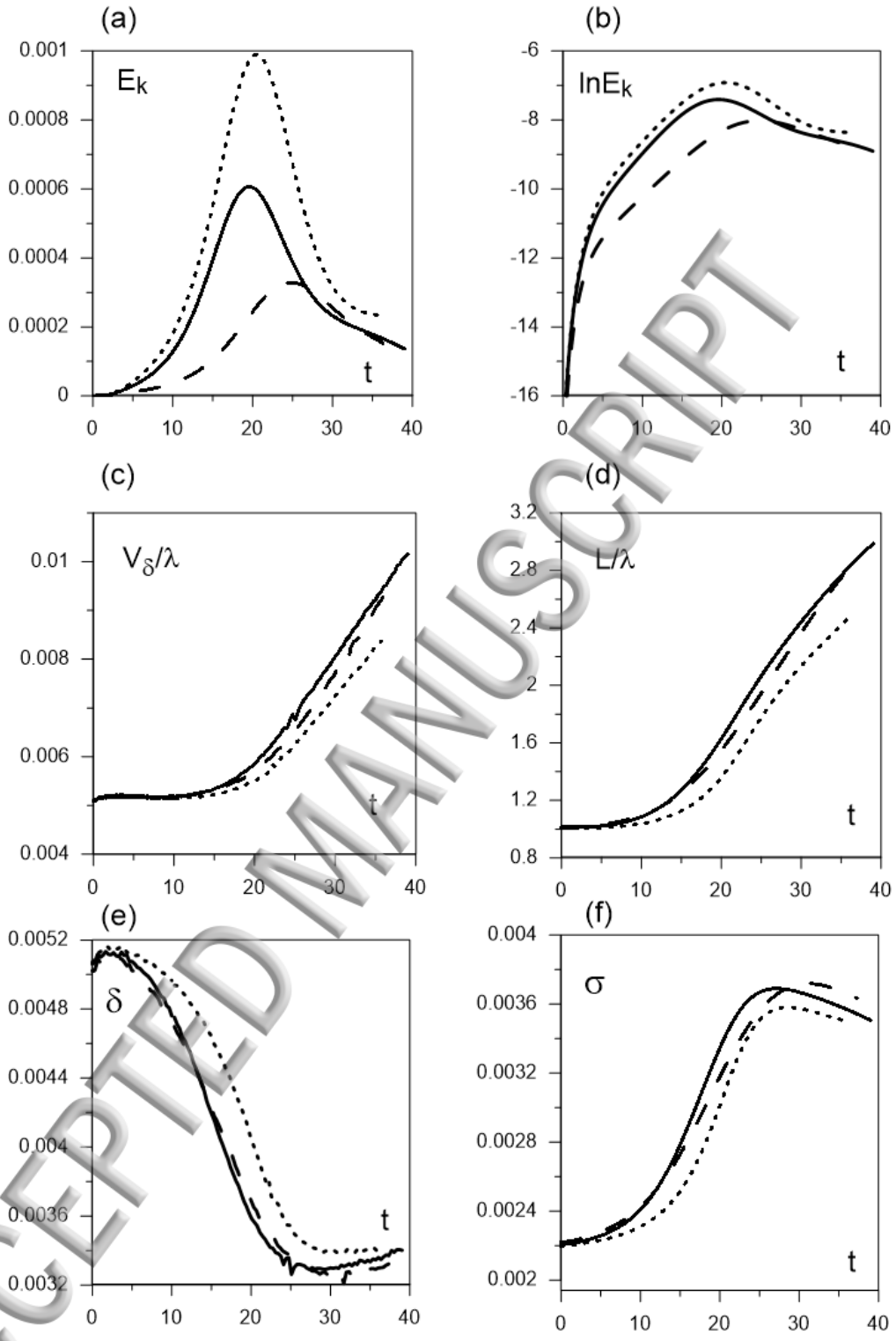

ACCEPTED MANUSCRIPT

FIG. 8. The time evolutions of the total kinetic energy (a) and of the logarithm of the kinetic energy (b), of the volume of the transition zone between the liquids (c) and the length of the interface (d), both scaled by the wavelength of the initial perturbation, λ, of the thickness of the interface (e), and of the surface tension coefficient (f). The data are obtained for $\delta_0 = 5.96 \cdot 10^{-3}$, A $= -0.5$, Ca $= 4 \cdot 10^{-5}$, Gr $= 0.1$, Re $= 100$, Pe $= 10^7$, and for three different wavenumbers, 2.86 (dotted line), 3.93 (solid line), and 5.03 (dashed line).

Taylor instability that develops at an infinitely thin interface between two immiscible liquids. The phase-field results are still far from the curves for the sharp immiscible interfaces, indicating that for an accurate reproduction of the immiscible results the calculations at even higher Peclet numbers are required. We also investigate the roles of the capillary parameter and the value of the initial interface thickness on the growth rates. The al-

This manuscript was accepted by Phys. Fluids. Click here to see the version of record.

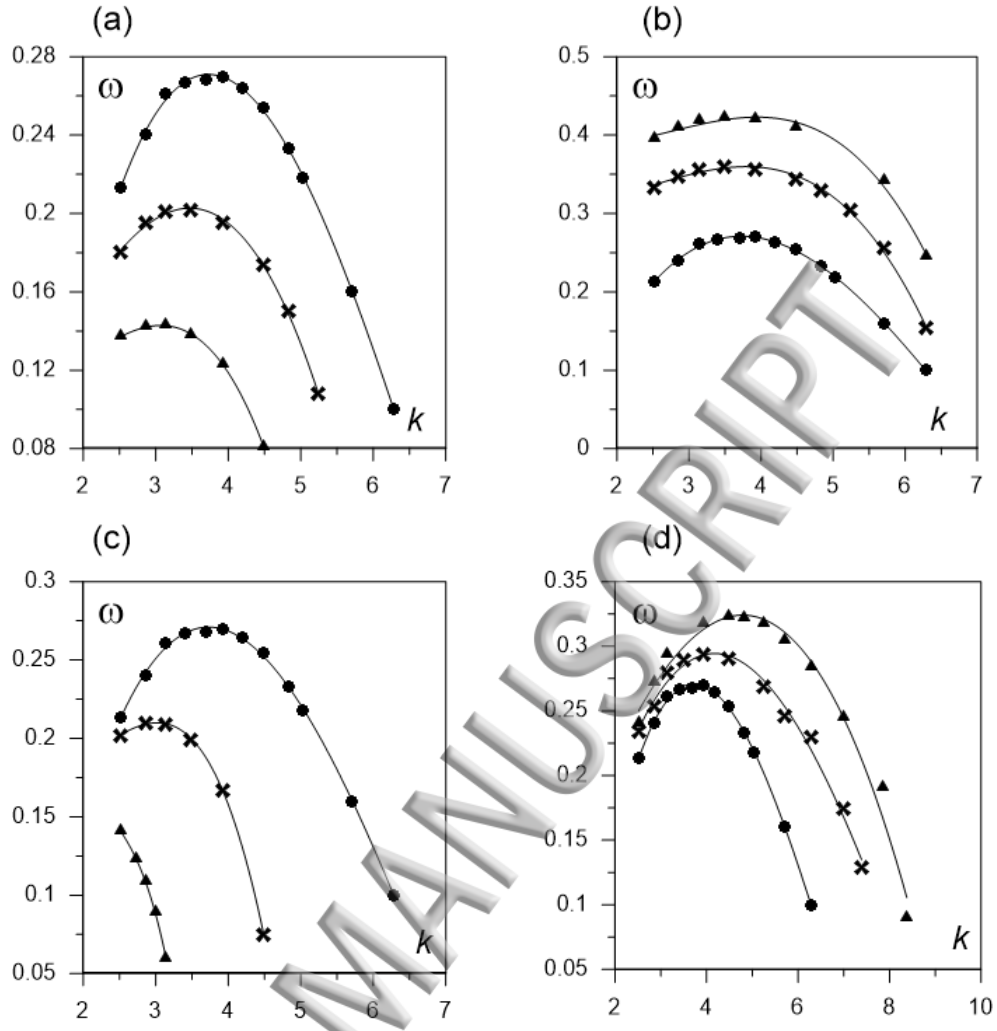

FIG. 9. The dependencies of the growth rate on the wavenumber are shown for (a) three different Grashof numbers (Gr = 0.1, circles, Gr = 0.08, crosses, and Gr = 0.06, triangles); (b) three different Reynolds numbers (Re = 100, circles, Re = 200, crosses, and Re = 400, triangles); (c) three different values of the capillary number (Ca = $4 \cdot 10^{-5}$, circles, Ca = $1.6 \cdot 10^{-4}$, crosses, and Ca = $6.4 \cdot 10^{-4}$, triangles); and (d) three different values of the Peclet number (Pe = 10^7, circles, Pe = 10^6, crosses, and Pe = 10^5, triangles). The base parameters for these calculations were $\delta_0 = 5.96 \cdot 10^{-3}$, A = −0.5, Gr = 0.1, Ca = $4 \cdot 10^{-5}$, Gr = 0.1, Pe = 10^7, and Re = 100, and one of the parameters was varied as set above.

teration of these parameters changes the surface tension of the interface, so we consider their independent variations and the simultaneous change of both parameters so that their ratio, that should be proportional to the surface tension coefficient,[38] remains constant. The curves of the growth rates obtained for the thinner boundaries lie closer to the theoretical results, showing the convergence of the phase-field results to the classical results. The change of the capillary parameter (by the same factor as the change of the initial interface thickness) had a weaker effect on the values of the growth rate.

VI. CONCLUSIONS

We study the isothermal evolution of a heterogeneous mixture of two slowly miscible liquids enclosed in a horizontal plane layer. We assume that at the initial time moment the two miscible liquids are brought into contact. The initial state of the mixture is thermodynamically unstable resulting in generation of the bilateral interfacial diffusion. We also assume that at the initial time moment the heavier liquid overlays the lighter liquid, which makes the initial configuration gravitationally unstable leading to the development of the Rayleigh-Taylor instability. The phase-field approach is used to examine the interaction of the diffusive and hydrodynamic evolution. In contrast with the other studies of the Rayleigh-Taylor instability, we, on one hand, consider the mixing in a heterogeneous mixture (with the clearly defined interfacial boundaries that are endowed with the surface tension), and, on the other hand, we examine the effects of the diffusive interpenetration of the mixture components.

We numerically model the transformation of the binary system until it reaches the state of thermodynamic and hydrodynamic equilibrium. The large difference in the convective and diffusive time scales results in the evolution that can be clearly split into two stages. At the initial stage, the diffusion role is weak, and the system

ACCEPTED MANUSCRIPT

This manuscript was accepted by Phys. Fluids. Click here to see the version of record.

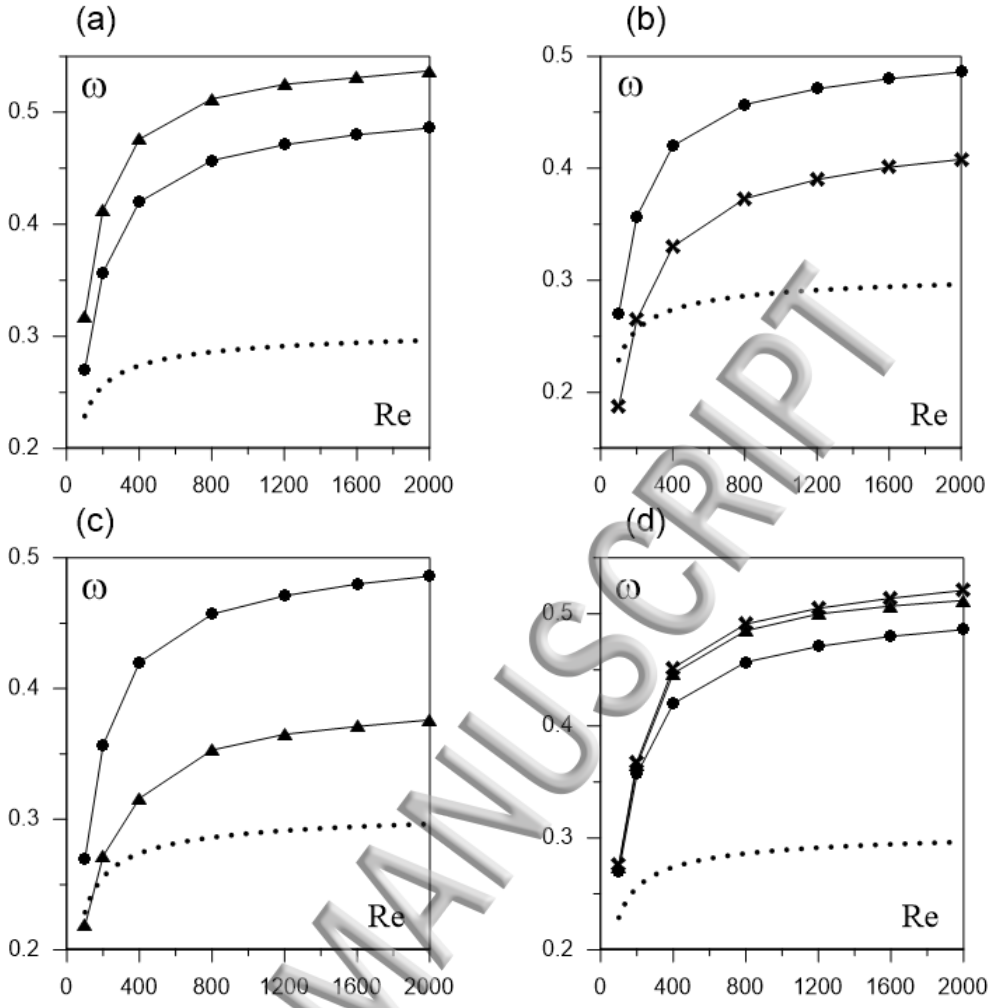

FIG. 10. The growth rates of the Rayleigh-Taylor instability are plotted as functions of the Reynolds number. The data are obtained for (a) two different Peclet numbers (Pe = 10^7, circles, and Pe = 10^5, triangles); and (b) two different capillary numbers (Ca = $4 \cdot 10^{-5}$, triangles, and Ca = $8 \cdot 10^{-5}$, crosses); (c) two different values of the initial interface thickness, $\delta_0 = 5.96 \cdot 10^{-3}$, circles, and $\delta_0 = 2.98 \cdot 10^{-3}$, triangles; and (d) three different values of the capillary parameter and interface thickness so that their ratio remains the same (Ca = $4 \cdot 10^{-5}$, $\delta_0 = 5.96 \cdot 10^{-3}$, circles, Ca = $8 \cdot 10^{-5}$, $\delta_0 = 0.0119$, square, and Ca = $1.6 \cdot 10^{-4}$, $\delta_0 = 0.0238$, crosses). The default parameters used for these curves were $k = 3.93$, $\delta_0 = 5.96 \cdot 10^{-3}$, A = -0.5, $Pe = 10^7$, Gr = 0.1, Re = 100, and Ca = $4 \cdot 10^{-5}$, and one or two parameters were varied as defined above. The dotted line depicts the results obtained from formula (19) that defines the growth rates for the Rayleigh-Taylor instability of an immiscible, infinitely thin interface, that is plotted for the value of the surface tension coefficient, $\sigma = 0.0035$, that corresponds to the value of the surface tension at the end of the period of the exponential growth.

primarily evolves to achieve the state of the hydrodynamic equilibrium (so that the system becomes gravitationally stable with the heavier liquid at the bottom). At the end of this stage the hydrodynamic motion ceases to exist, so the second stage corresponds to the much slower inter-diffusion of the liquids. Nevertheless, our analysis shows that both stages are substantially affected by the diffusion and convection effects.

We trace the development of a disturbance defined by a single value of the wave-number. Only the long-wave perturbations, with the wavelengths comparable to the height of the plane layer, are examined. The growth of the perturbations was always restricted by the walls of the layer, and e.g. the turbulent regimes of the instability are never reached in our calculations.

At the initial stage, we can clearly identify the period of the exponential growth of the kinetic energy of the hydrodynamic flow, and the period of the fast changes of other physical quantities that may also be well fitted by the exponential time dependencies. This period seems to be well explained by the linear stability theory, although, through the full non-linear analysis of the problem, we found that the interface deformation results in the interface thinning, so the thickness of the interface changes in time following the same exponential time law as the development of the Rayleigh-Taylor instability. The interface thinning leads to the growth of the surface tension coefficient, altering the growth rates of the unstable modes and the peak values of the total energy of the kinetic energy. This effect is overlooked in the linear stability analyses.

We found that the growth rates for the development of the Rayleigh-Taylor instability are higher for the mixture with the greater density contrasts. The development of

ACCEPTED MANUSCRIPT

This manuscript was accepted by Phys. Fluids. Click here to see the version of record.

the instability is slowed down by the viscous and capillary forces. The effect of diffusion on the development of the early stage of the evolution of a binary system is primarily revealed through its influence on the interface thickness, and hence on the surface tension coefficient. In particular, we found that the development of the instability at the higher Peclet numbers occurs even slower due to the stronger interface stretching that ultimately limits the growth of the hydrodynamic modes. The increase of the Peclet number and the reduction of the initial interface thickness lead to the clear convergence of the results to the classical curves obtained for the case of immiscible infinitely thin interfacial boundaries.

We also found that the interface stretching, i.e. enlargement of the contact area of the phases results in substantial reduction of the time needed for the transition of the binary system to the state of thermodynamic equilibrium. In the end of the first convection stage of the evolution the binary mixture reaches the state that is much closer to the final state of the thermodynamic equilibrium as compared with the initial state of the system, and as compared with the state that the system might achieve through the purely diffusive transformation (e.g. if the initial state of the system corresponds to the gravitationally stable configuration).

We found that the effect of the interface stretching depends on the initial thickness of the interface, so it becomes less pronounced if the interface is thinner.

Finally, on the basis of the conducted study we would like to draw some correspondence between the standard phenomenological parameters and the phenomenological parameters that are introduced by the phase-field theory. In particular, the dimensional value of the surface tension coefficient may be obtained from our results as $\sigma_{dim} = \rho_* \mu_* L_* \sigma$. The use of this formula remains however impossible without the knowledge of the typical value of the chemical potential. We suggest using the latter formula in the opposite way, in order to obtain the typical value of the chemical potential, μ_*. In our calculations, the surface tension coefficient, σ, varied over the evolution of the system, and was different for the runs with the different capillary numbers and the initial interface thicknesses. Nevertheless, one may say that the typical value of this coefficient was $\sigma \sim 10^{-3}$. For the typical value of the density we take $\rho_* \sim 10^3\, kg/m^3$ and for the typical length scale we assume $L_* \sim 10^{-2} m$. The dimensional value of the surface tension coefficient depends on the particular binary mixture, although the rough range for the values for this coefficient is $(10^{-2}..10^{-5})\, N/m$ (the greater value would be more typical for an immiscible liquid/liquid interface, and the smaller value is more typical for miscible interfaces[23]). Summarising these parameters, we conclude that the typical value of the chemical potential varies in the range $(10^{-3}..1)\, J/kg$. This estimate may now be used for conducting the more practically relevant calculations for the binary mixtures that experience simultaneous thermo- and hydrodynamic changes. The latter estimate could be also used to say that the typical density contrast that characterises the examined binary mixture is of the order (1..10).

ACKNOWLEDGMENTS

The financial support of the Russian Foundation for Basic Research (Grant No. 16-5110079), and the Royal Society (Ref. IE160277) is gratefully acknowledged. The numerical calculations were performed using the 'Uran' supercomputer of the IMM UB RAS.

[1] M. R. Shahnazari, I. Ashtiani, and A. Saberi, Phys. Fluids **30**, 034106 (2018).
[2] M. Zargartalebi and J. Azaiez, Phys. Fluids **30**, 024105 (2018).
[3] G. H. Wolf, Phys. Fluids **30**, 021701 (2018).
[4] E. Khlebnikova, E. Ivashkina, and I. Dolganova, Chemical Engineering and Processing: Process Intensification **120**, 234 (2017).
[5] G. Taylor, Proceedings of the Royal Society A **201**, 192 (1950).
[6] R. Bellman and R. H. Pennington, Quarterly of Applied Mathematics **12**, 151 (1954).
[7] H. W. Emmons, C. T. Chang, and B. C. Watson, Journal of Fluid Mechanics **7**, 177 (1960).
[8] M. Ratafia, Physics of Fluids **16**, 1207 (1973).
[9] P. Kurowski, C. Misbah, and S. Tchourkine, Europhys. Lett. **29**, 309 (1995).
[10] P. F. Linden, J. M. Redondo, and D. L. Youngs, Journal of Fluid Mechanics **265**, 97 (1994).
[11] D. M. Snider and M. J. Andrews, Phys. Fluids **6**, 3324 (1994).
[12] P. Ramaprabhu and M. J. Andrews, Journal of Fluid Mechanics **502**, 233 (2004).
[13] N. Mueschke, M. J. Andrews, and O. Schilling, Journal of Fluid Mechanics **567**, 27 (2006).
[14] N. Mueschke, O. Schilling, D. L. Youngs, and M. J. Andrews, Journal of Fluid Mechanics **632**, 17 (2009).
[15] H. Aref and G. Tryggvason, Physical Review Letters **62**, 749 (1989).
[16] M. Chertkov, Physical Review Letters **91**, 115001 (2003).
[17] A. W. Cook and P. E. Dimotakis, Journal of Fluid Mechanics **443**, 69 (2001).
[18] Y.-N. Young, H. Tufo, A. Dubey, and R. Rosner, Journal of Fluid Mechanics **447**, 377 (2001).
[19] M. Payr, S. H. Vanaparthy, and E. Meiburg, Journal of Fluid Mechanics **525**, 333 (2005).
[20] N. Mueschke and O. Schilling, Physics of Fluids **21**, 014106 (2009).
[21] N. Mueschke and O. Schilling, Physics of Fluids **21**, 014107 (2009).
[22] D. D. Joseph and Y. Y. Renardy, *Fundamentals of two-fluid dynamics. Part II: Lubricated transport, drops and miscible liquids* (Springer-Verlag, Berlin, 1993).
[23] A. Vorobev, Current Opinion in Colloid & Interface Science **19**, 300 (2014).
[24] L. D. Landau and E. M. Lifshitz, *Fluid Mechanics. (Volume 6 of Course of Theoretical Physics)* (Butterworth-Heinemann, Elsevier, 1987).
[25] F. B. Hicks, T. C. V. Vechten, and C. Franck, Physical Review E **55**, 4158 (1997).
[26] A. Vailati and M. Giglio, Physical Review E **58**, 4361 (1998).
[27] K. Jamshidi-Ghaleh, M. T. Tavassoly, and N. Mansour, J Phys D: Appl Phys **37**, 1993 (2004).
[28] D. J. Korteweg, Archives Nerlandaises des Sciences exactes and Naturelles, Sries II **6**, 1 (1901).
[29] J. S. Rowlinson, J. Stat. Phys. **20**, 197 (1979).
[30] Y. B. Zeldovich, Zh. Fiz. Khim. **23**, 931 (1949).
[31] J. W. Cahn and J. E. Hilliard, Journal of Chemical Physics **28**, 258 (1958).
[32] J. Lowengrub and L. Truskinovsky, Proceedings of the Royal Society A **454**, 2617 (1998).
[33] D. Jasnow and J. Vinals, Phys. Fluids **8**, 660 (1996).
[34] D. Jacqmin, Journal of Computational Physics **155**, 96 (1999).
[35] H. Ding, P. D. M. Spelt, and C. Shu, Journal of Computational Physics **226**, 2078 (2007).
[36] A. Celani, A. Mazzino, P. Muratore-Ginanneschi, and L. Vozella, Journal of Fluid Mechanics **622**, 115 (2009).
[37] A. Vorobev, Physical Review E **82**, 056312 (2010).

ACCEPTED MANUSCRIPT

This manuscript was accepted by Phys. Fluids. Click here to see the version of record.

[38] A. Khenniene and A. Vorobev, Physical Review E **88**, 022404 (2013).
[39] A. Vorobev, A. Ivantsov, and T. Lyubimova, European Physical Journal E **40** (2017).
[40] R. Xie and A. Vorobev, J. Colloid Interface Sci **464**, 48 (2016).
[41] A. Vorobev and A. Boghi, J. Colloid Interface Sci **482**, 193 (2016).
[42] A. Vorobev and E. Khlebnikova, International Journal of Heat and Mass Transfer **125**, 801 (2018).
[43] P. J. Flory, *Principles of Polymer Chemistry* (Cornell University Press, 1953).
[44] In the case of the negligible gravity and capillary effects the shape of the phase diagram, defined by the curves of coexistence of two phases, can be obtained by solving the equation, $\mu_0 = df_0/dC = 0$. For the chemical potential derived from the Landau free energy function (4) the solutions of this equation can be easily obtained analytically, namely, $C_{eq} = \pm\sqrt{-a/2b}$.
[45] A. Vorobev, D. Lyubimov, and T. Lyubimova, Physical Review E **95**, 022803 (2017).
[46] Substitution of the expression for the chemical potential into the equation for the species balance would show that the barodiffusion does not affect the mass transport in the bulk layer. Nevertheless, this term still affects the boundary conditions thus influencing the long term evolution of the fluid system, when the influence of the boundary values propagates into the main layer. Although, for the problem of the stability of an interfacial boundary the influence of this term should be minimal.
[47] The parameter A sets the values of the concentration for the equilibrium state (see figure 1): the system is homogeneous in equilibrium (the liquids are fully miscible) if $A > 0$, and the system remains heterogeneous in equilibrium (the liquids are partially miscible) if $A < 0$. For the free energy function (5) the shape of the phase diagram is similar, with the equilibrium value $C_{eq} = \pm 0.388$ at $A = -0.5$. In addition, the parameter A determines the value of the equilibrium interface thickness (for expression (4), $\delta_{eq} = \sqrt{-Ca/A}$), and the diffusion rate (the effective diffusion coefficient outside of the interfacial layer is given by $D = \alpha \frac{\mathrm{d}\mu}{\mathrm{d}C} \sim \alpha(2A + 12C^2)$). The data in this work is obtained for the fixed value of the parameter A. The results however should not be qualitatively different for other negative values of the parameter A. The results although can be stronger different, resembling the case of the Fickian diffusion, for the positive values of the parameter A.
[48] The level of mixing ('mixedness') on different scales, e.g. the break-up of the phases into smaller domains and the further interpenetration of the phases into each other, can be measured by the Mix-Norm characteristics that was introduced by Mathew et al.[51]. In the current work we however are primarily interested in the mixing on molecular level. The degree and the rate of the molecular-level mixing can be well characterised by the average concentrations within each phase, and hence the Mix-Norm was not calculated.
[49] The linear stability of a miscible interface is always based on the approximation of a 'frozen' interface boundary,[9,38] thus effectively neglecting the slow diffusive smearing of the boundary in comparison with the fast exponential growth of the unstable modes.
[50] S. Chandrasekhar, *Hydrodynamic and Hydromagnetic Stability* (Clarendon Press, Oxford, 1961).
[51] G. Mathew, I. Mezic, and L. Petzold, Physica D **211**, 23 (2005).

ACCEPTED MANUSCRIPT

ACCEPTED

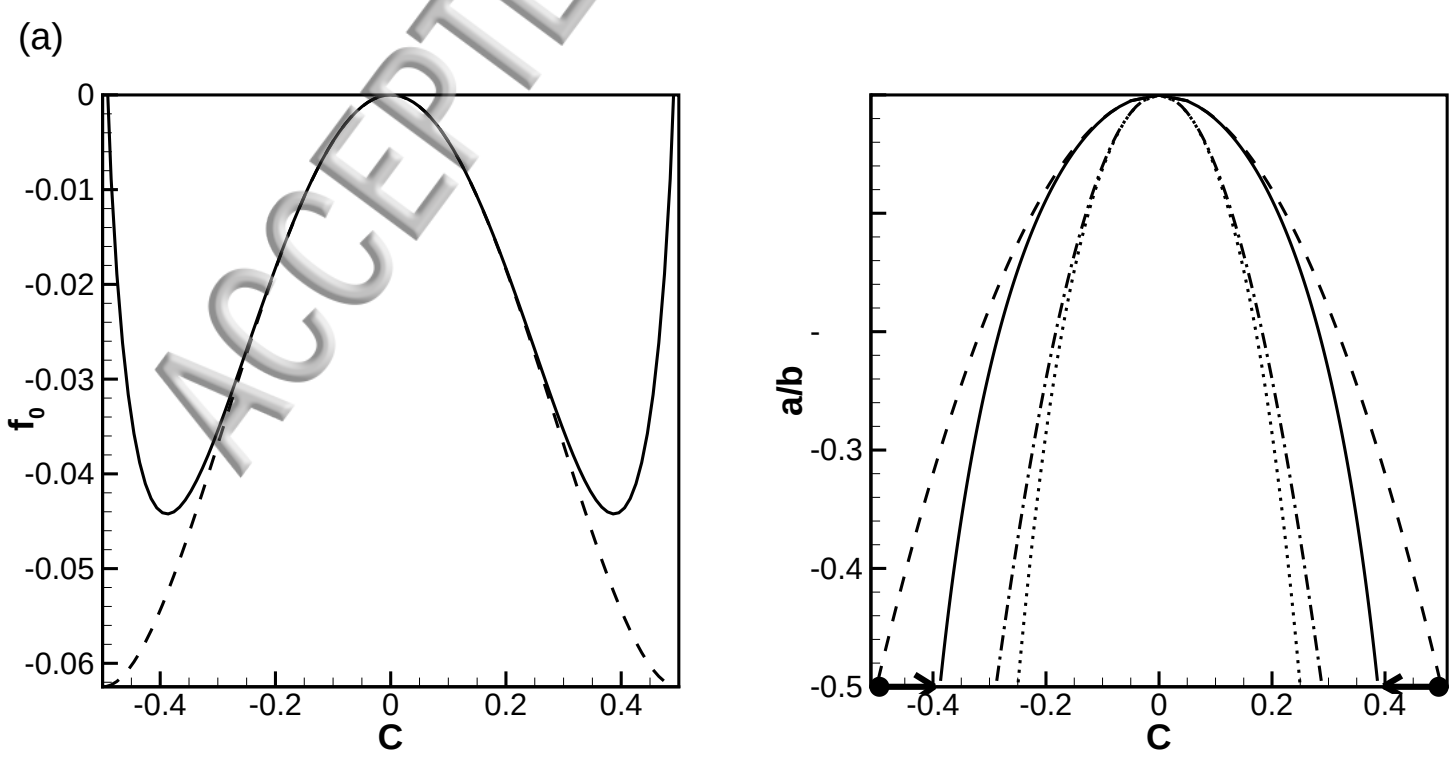
(a)
0
-0.01
-0.02
-0.03
-0.04
-0.05
-0.06
f_0
-0.4
-0.2
0
0.2
0.4
c
a/b
-0.3
-0.4
-0.5
-0.4
-0.2
0
0.2
0.4
c

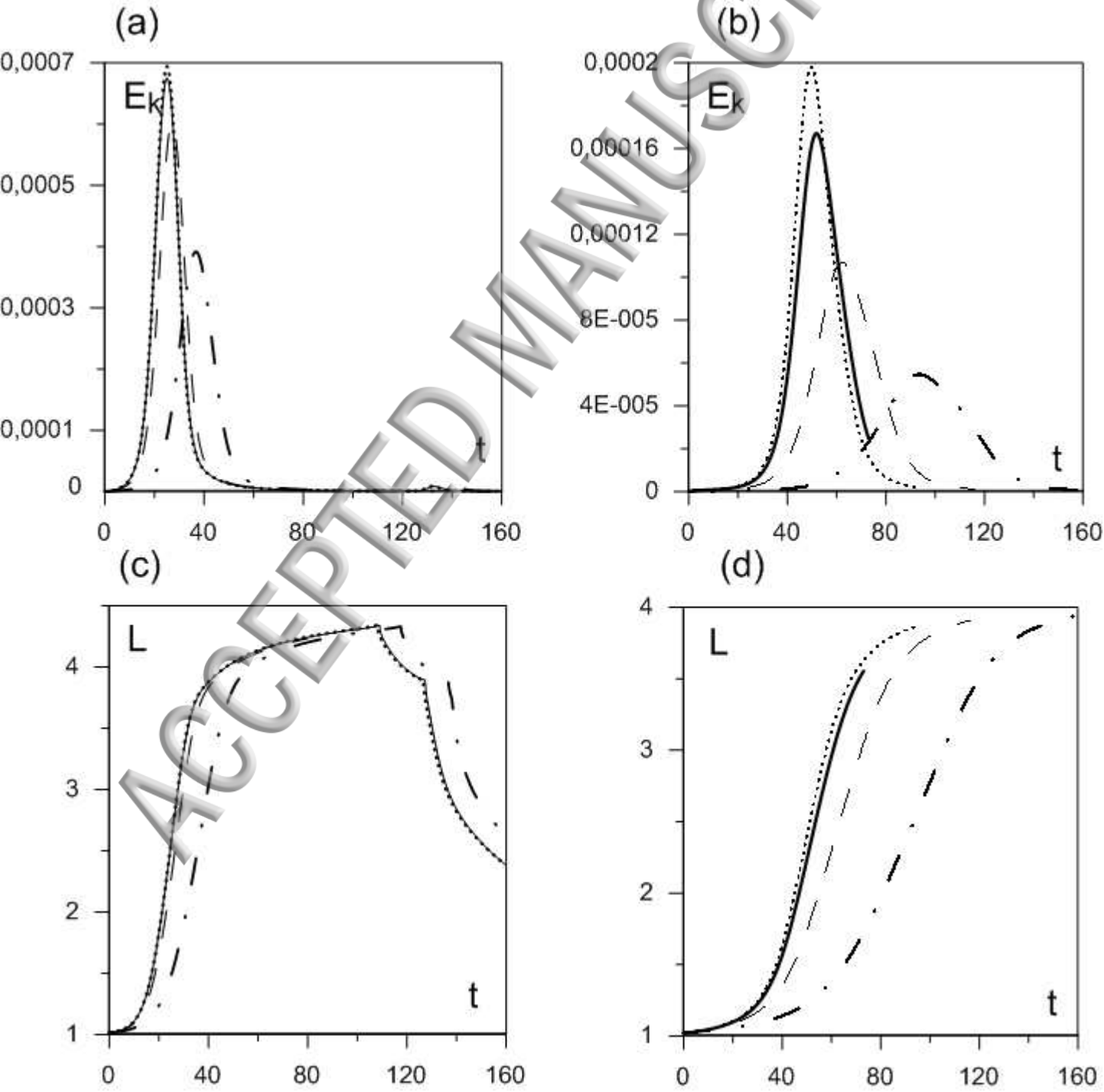

ACCEPTED MANUSCRIPT

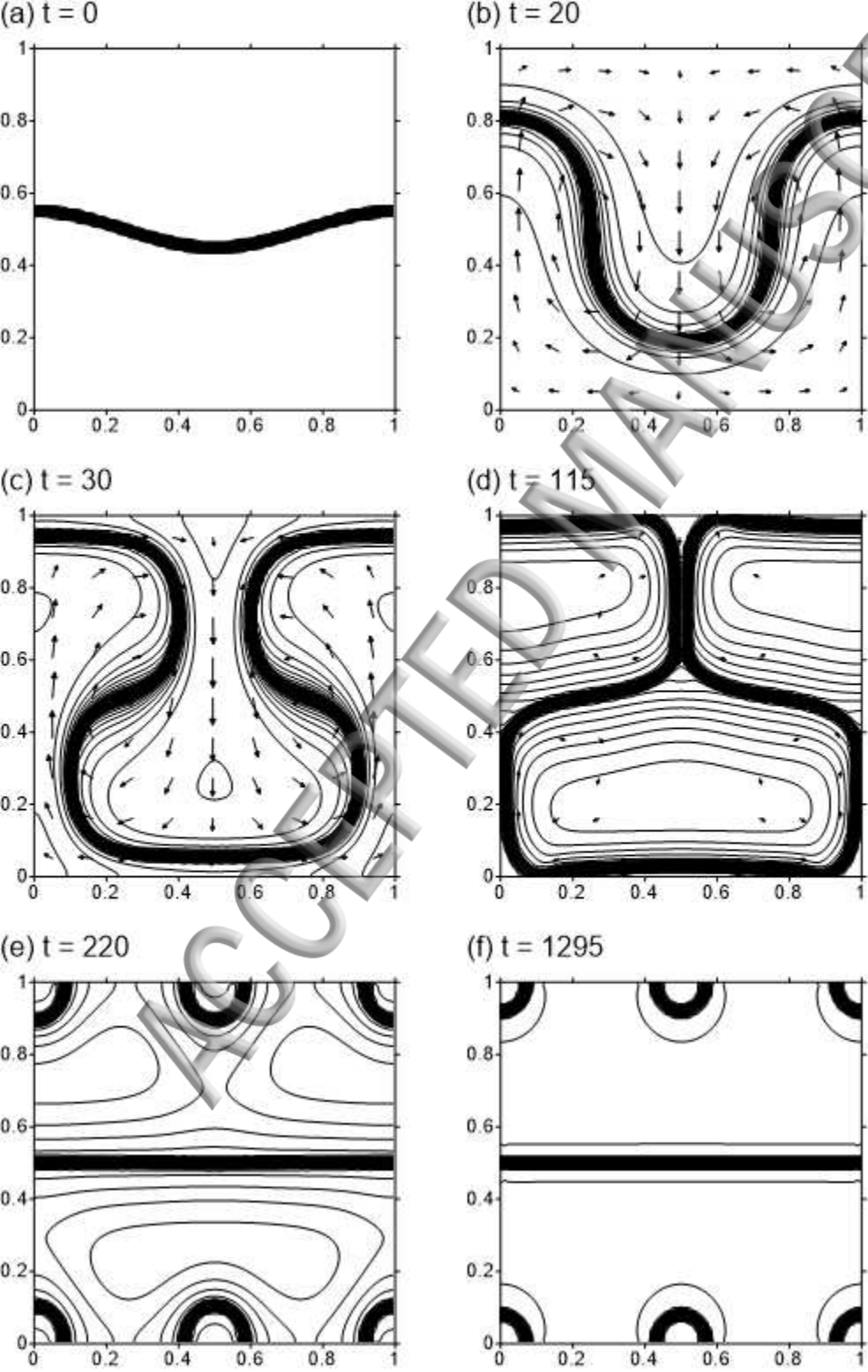

ACCEPTED MANUSCRIPT

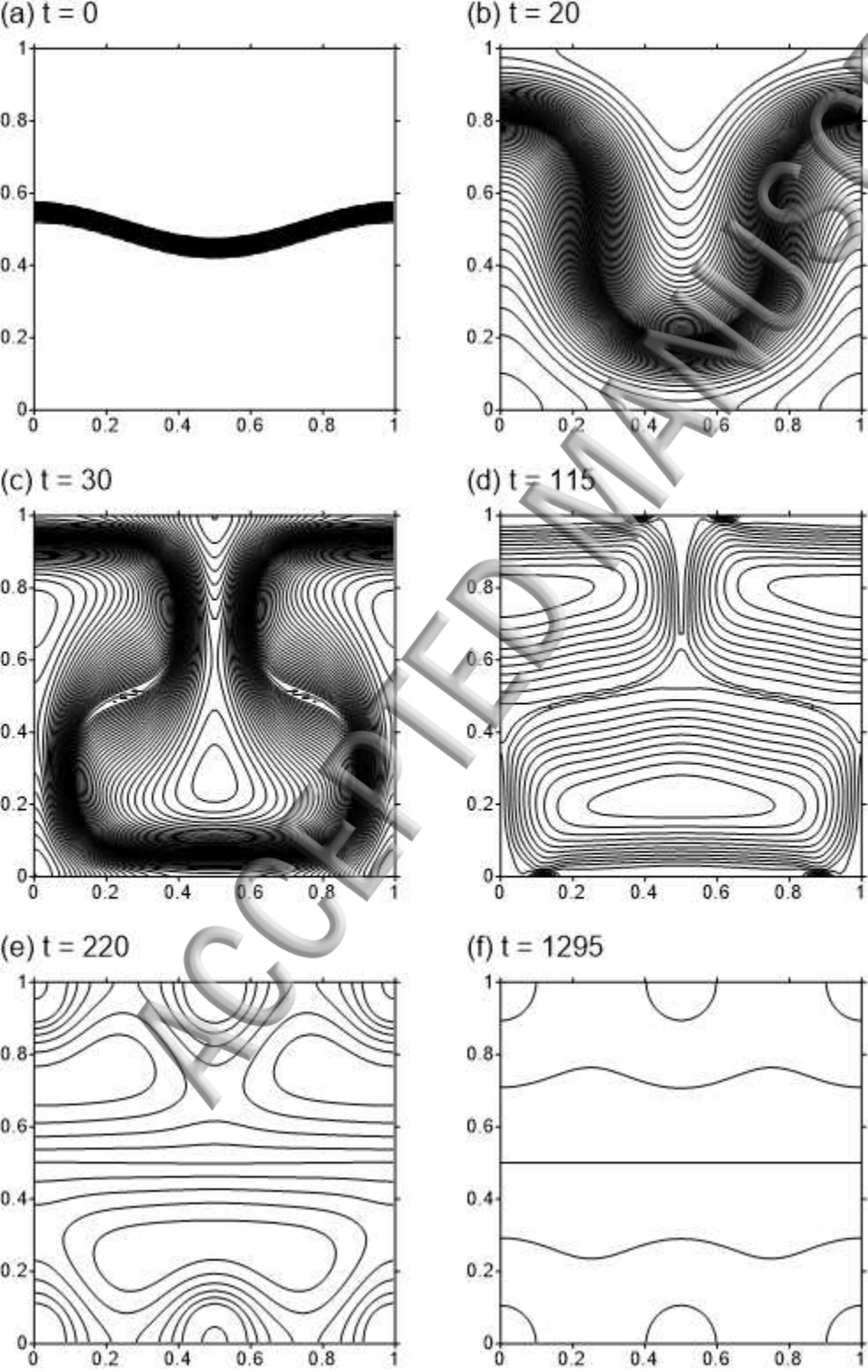

ACCEPTED MANUSCRIPT

This manuscript was accepted by Phys. Fluids. Click here to see the version of record.

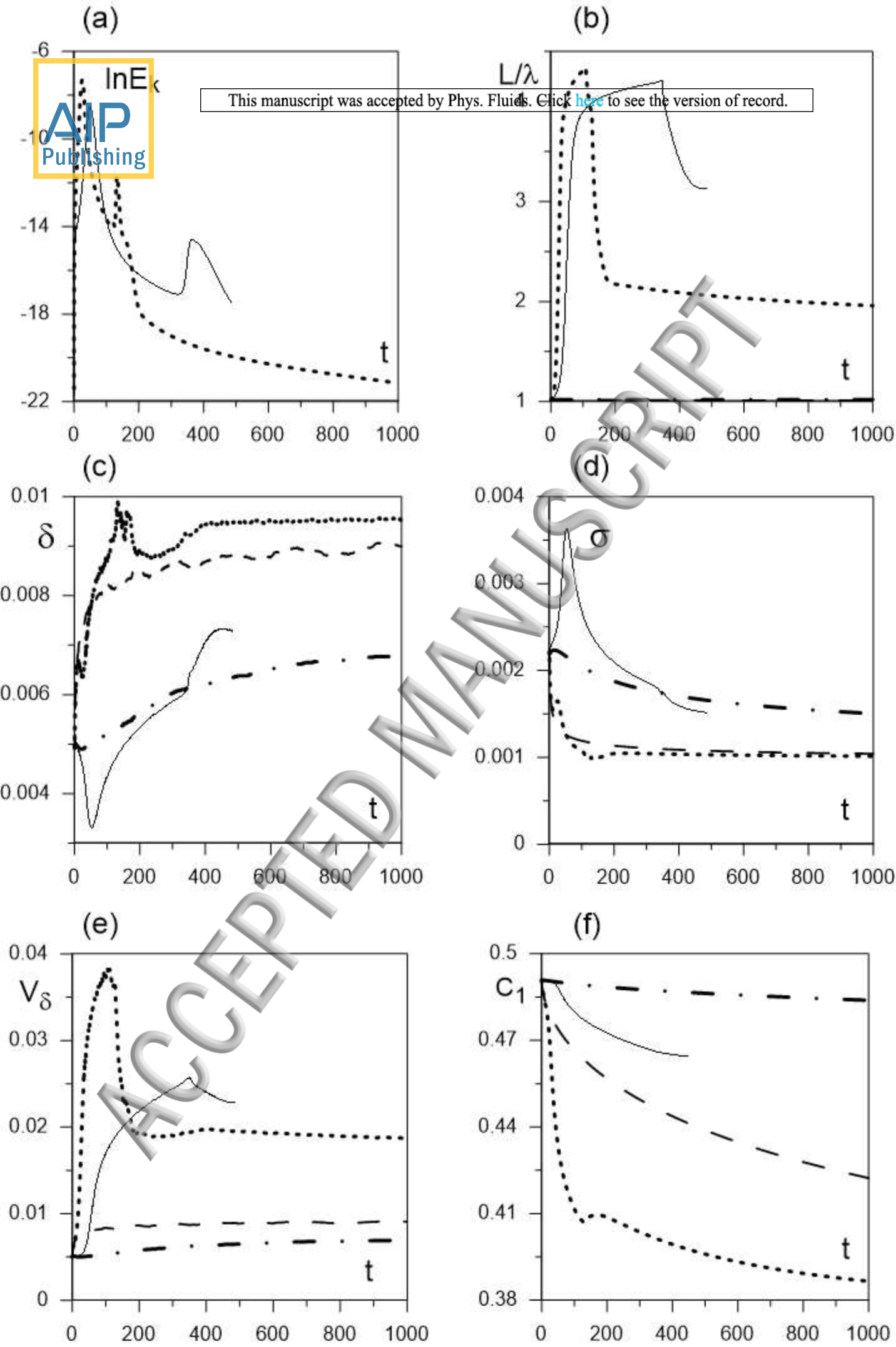

ACCEPTED MANUSCRIPT

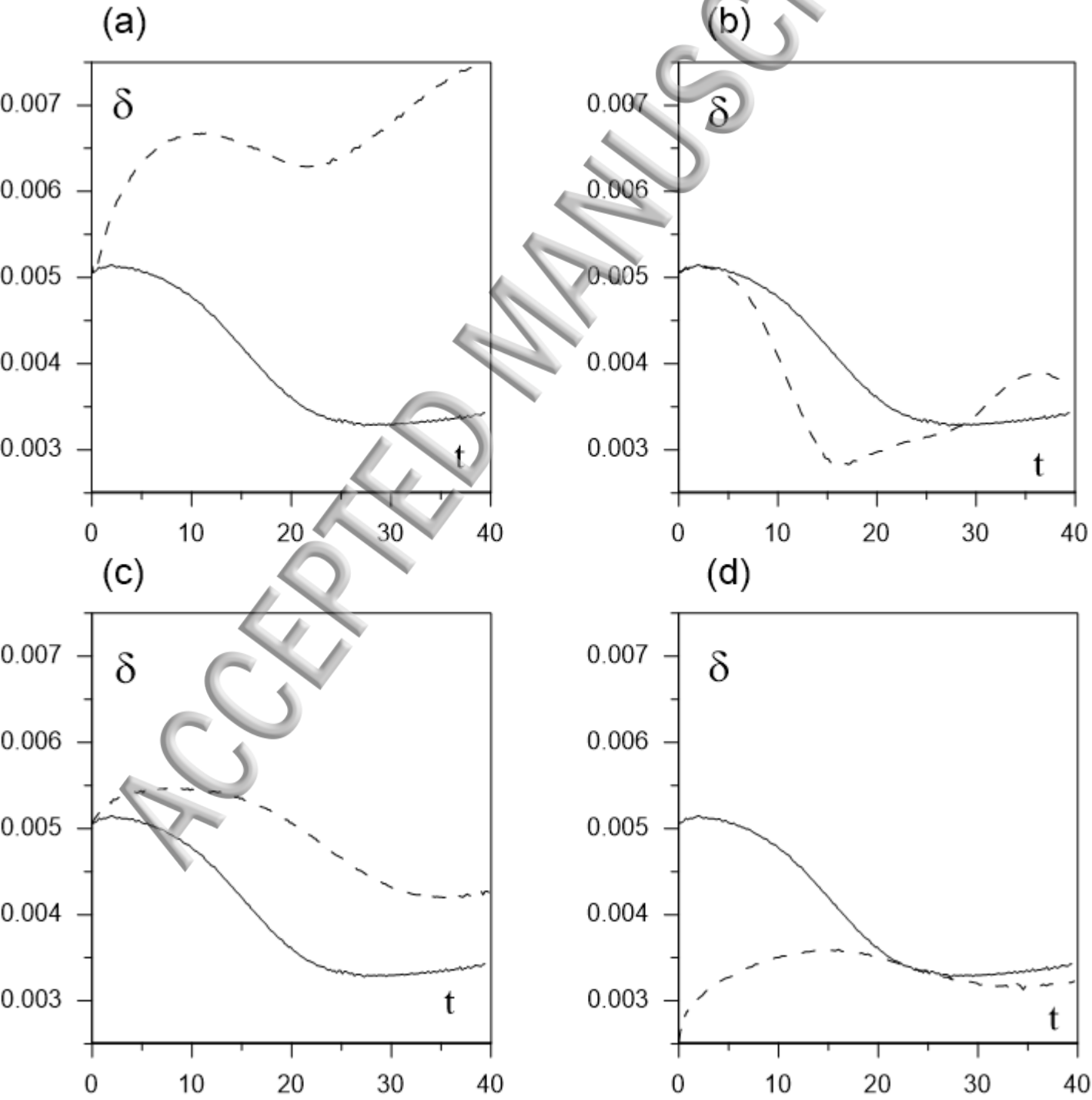

ACCEPTED MANUSCRIPT

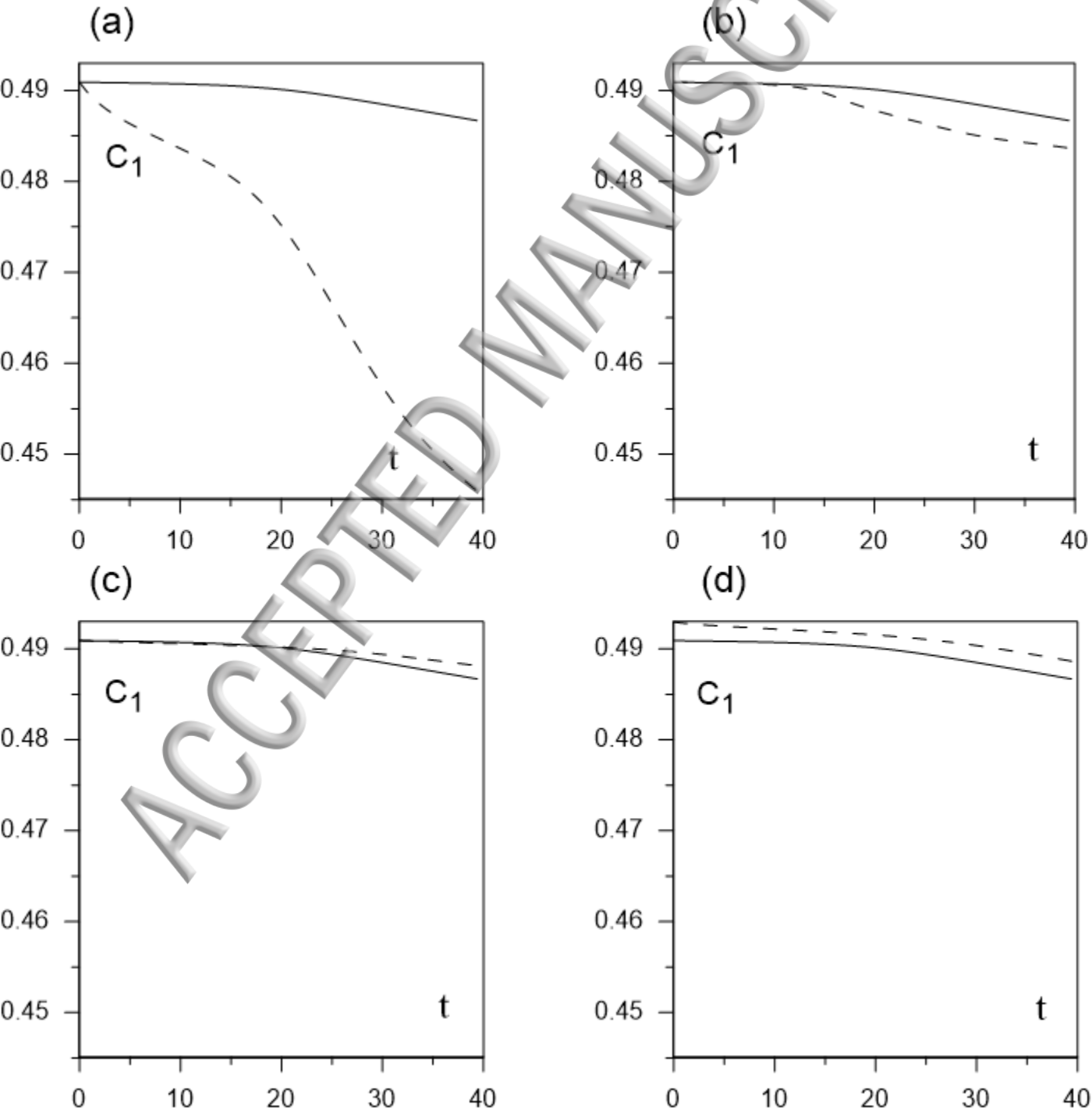

ACCEPTED MANUSCRIPT

AIP Publishing
This manuscript was accepted by Phys. Fluids. Click here to see the version of record.

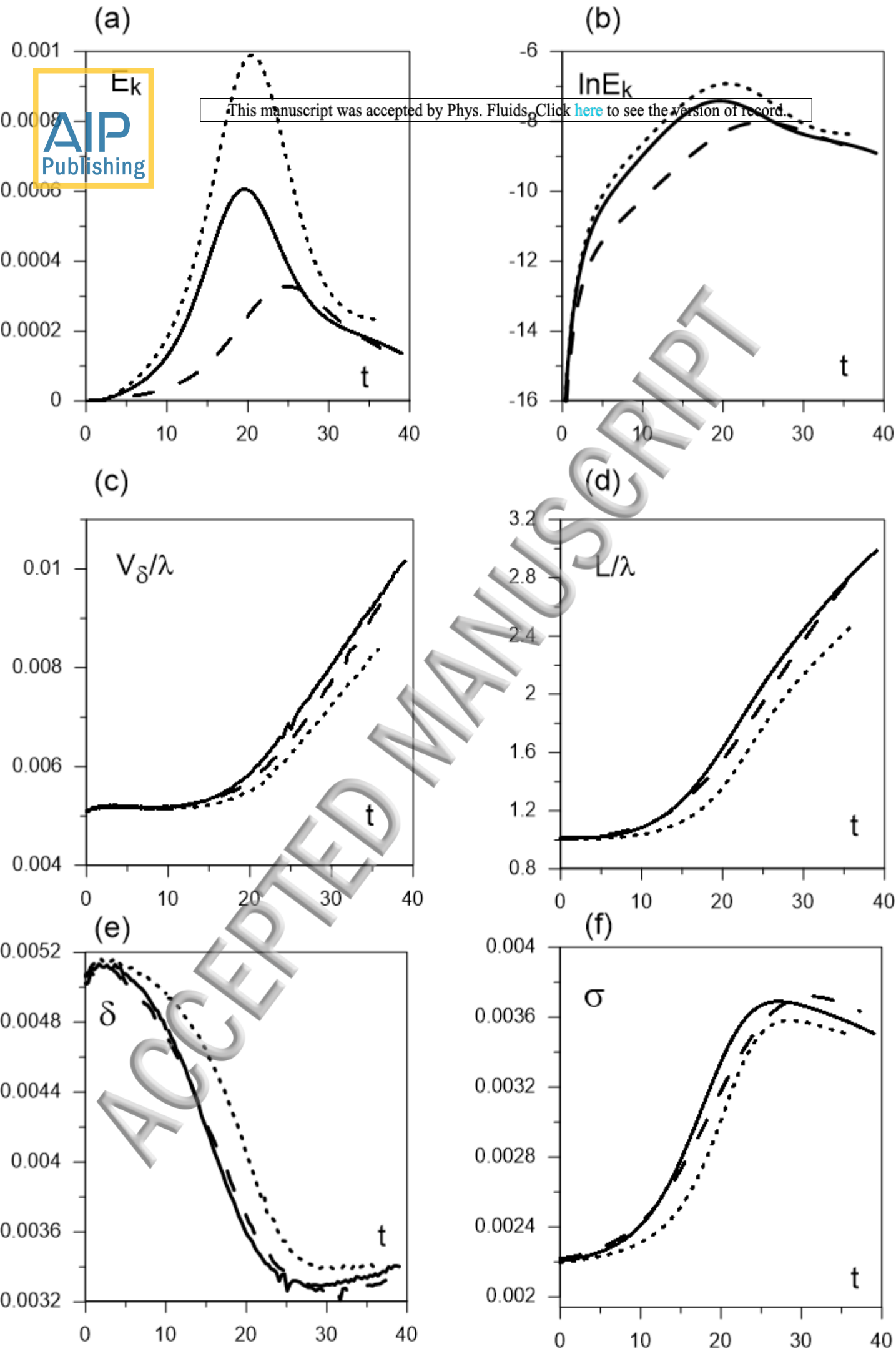

ACCEPTED MANUSCRIPT

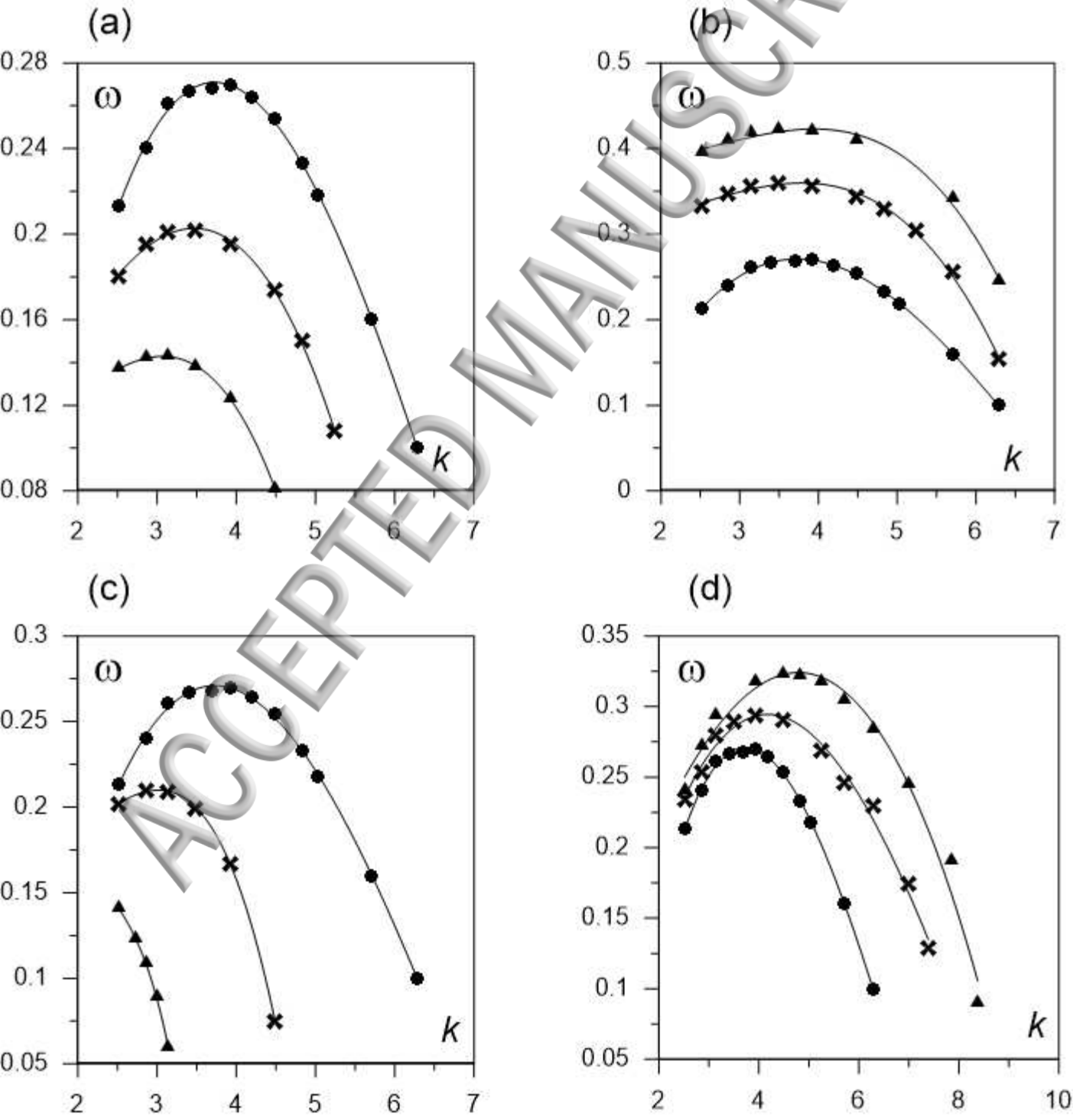

ACCEPTED MANUSCRIPT

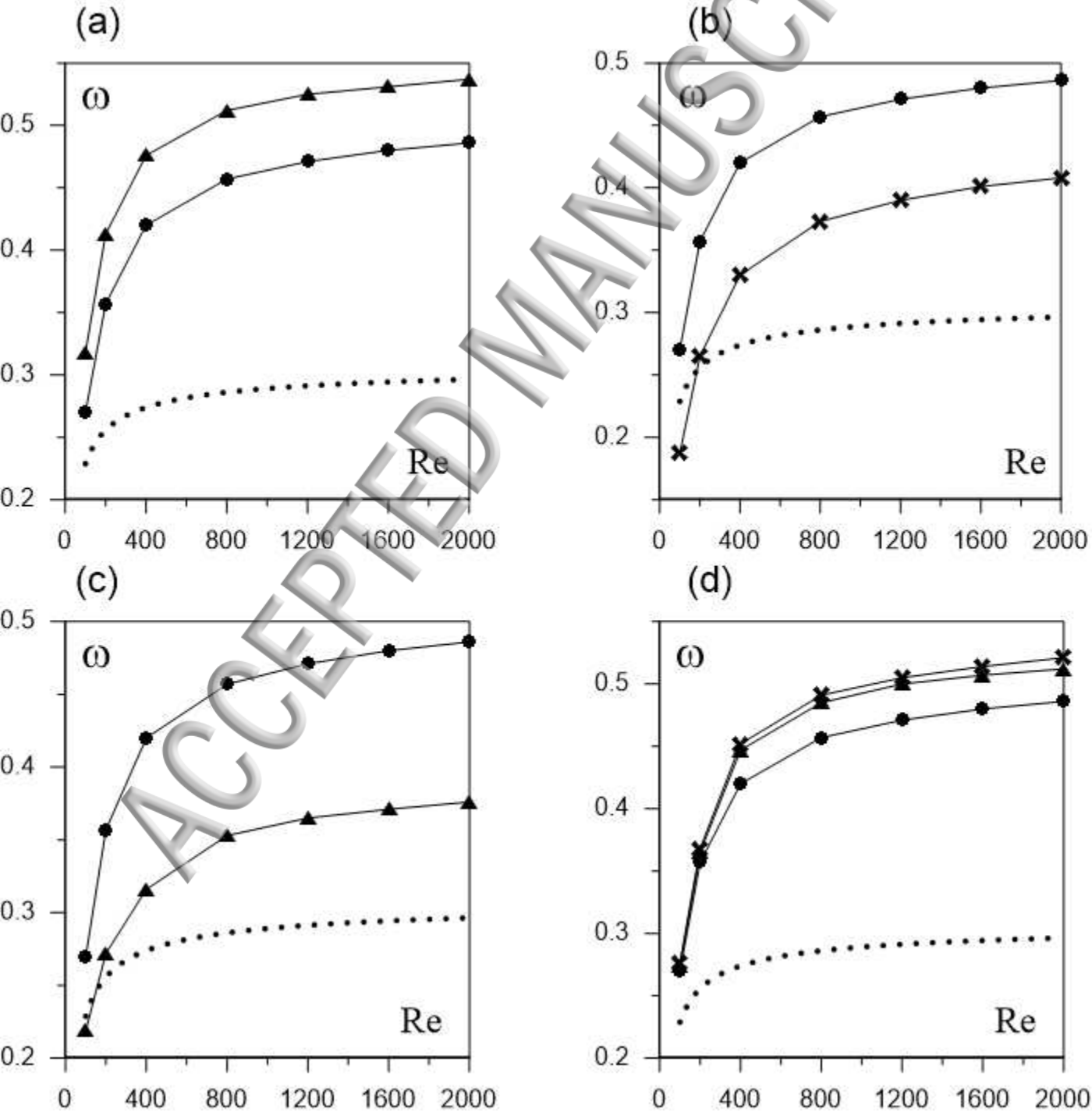

ACCEPTED MANUSCRIPT